13

Effects of the Tibetan Plateau

Michio Yanai and Guo-Xiong Wu

The Tibetan Plateau (Qinghai–Xizang Plateau) extends over the latitude–longitude domain of 25–45°N, 70–105°E, with a size of about one-quarter of the Chinese territory and a mean elevation of more than 4,000 m above sea level (Figure 13.1, color section). Surface elevation changes rapidly across the boundaries of the Plateau, especially the southern boundary, and strong contrasts exist between the western and eastern parts in land surface features, vegetation, and meteorological characteristics (e.g., Ye and Gao, 1979b; Smith and Shi, 1995). At these altitudes the mass of the atmosphere over the surface is only 60% that at sea level. Because of the lower densities, various radiative processes over the Plateau, particularly in the boundary layer, are quite distinct from those over lower elevated regions (e.g., Liou and Zhou, 1987; Smith and Shi, 1992; Shi and Smith, 1992). Therefore, the Tibetan Plateau exerts profound thermal and dynamical influences on atmospheric circulation.

13.1 INTRODUCTION

Before the 1950s, most of the studies concerned with the influence of large-scale topography upon atmospheric circulation and climate focused on its mechanical aspects. Queney (1948) summarized the studies on airflow over mountains and brought forward three critical scales to distinguish different mountain waves by using linearized equations. He showed that gravity waves, inertial gravity waves, or Rossby waves will be forced when atmospheric current flows over mountains with various spatial scales. In the early 1950s, Bolin (1950) and Yeh (1950) suggested that the Tibetan Plateau splits the westerlies into two branches in winter and thus favors of the generation of the Great Trough over east Asia. The numerical simulations based on a new atmospheric model developed by Charney and Eliassen (1949) also concentrated on understanding the mechanical forcing of large-scale

B. Wang (ed.), *The Asian Monsoon*.

topography on the formation of mean troughs and ridges in the mid-latitude westerliers.

In 1957, Yeh *et al.* and Flohn respectively found that the Tibetan Plateau is a heat source to the atmosphere in summer. Since then the temporal and spatial distributions of the heating field over the Plateau and their impacts on weather and climate have become an important research field in meteorology. Earlier, the thermal influences of the Plateau upon atmospheric circulation were inferred from: (1) the shift of the mid-tropospheric westerly jet stream from the south side to the north side of the Plateau in early summer; (2) the presence of a huge warm-core anticyclone in the upper troposphere centered over the Plateau in summer; and (3) the pronounced diurnal variations in the surface meteorological elements on and along the periphery of the Plateau.

13.1.1 The jet stream

The earliest work that related the presence of the Himalayas to the onset of the summer monsoon was that of Yin (1949), a Burmese meteorologist visiting the University of Chicago and conducting research with Herbert Riehl. Yin recognized the westward shift of a trough, originally located to the east of India, in summer. He found that this movement is comparatively rapid and coincides with the 'burst of the monsoon' over India. The movement of the trough is explained as being due to 'changes in the long-wave pattern brought about by the presence of the Himalayan mountain complex combined with seasonal variation in the latitude of the circumpolar jet stream of the northern hemisphere.' The work of Yin was included in the textbook *Tropical Meteorology* by Riehl (1954) with an illustration (Yin, figure 6) of splitting and shifting of the westerly jet stream from the south side to the north side of the Tibetan Plateau. (Also, it is interesting to note that T. C. Yeh (i.e., Duzheng Ye), another visitor to the University of Chicago and Riehl's colleague, published his famous theoretical paper on dispersion of Rossby waves (Yeh, 1949) in the same year as Yin's.)

In 1951, Murakami published a paper entitled, 'Mechanism of Tsuyu-Ake (end of Baiu)'. In this paper, he showed splitting of the jet stream over Japan during Baiu (Meiyu in China) and the disappearance of the southern branch at the end of the Baiu season. The work of Yin and Murakami were followed by Suda and Asakura (1955) and Dao and Chen (1957). They showed that the onset of Baiu (Meiyu) and the south-west monsoon coincides with the time of the jet stream shifting from the south side to the north side of the Tibetan Plateau.

The role of the Tibetan Plateau on the withdrawal of the Asian monsoon has also been studied. Staff Members of Academia Sinica (1957) described that the sudden shift of jet stream from the north of Tibet (40°N) to the south (32°N) occurred in mid-October of 1956 along 125°E. Yeh *et al.* (1959) discussed the abrupt change of the upper air circulation over the northern hemisphere in June and October. The southward retreat of the jet stream around Tibet in October was shown by cross sections. Matsumoto (1988, 1990) studied the withdrawal of the Indian summer monsoon and its relation to the seasonal transition from summer

to autumn over east Asia. He described sudden temperature drops over the Eurasian continent in late September and October, which coincided with the sudden southward shift of the jet steam around the Tibetan Plateau.

13.1.2 Warm anticyclone

During the Second World War, a study of pilot-balloon data above northern India in summer showed the shift from westerlies to easterlies and the increase of easterlies with height. Considering the thermal wind relation, the presence of a warm anticyclone north of the Himalayas in the 300–100-hPa layer was inferred (Flohn, 1981). After the war, Flohn investigated the surface and upper air data and established the presence of the warm anticyclone on the Tibetan Plateau. He further pointed out the concurrent occurrence of 'reversal' of meridional temperature gradient south of the Himalayas and the onset of the Indian monsoon (Flohn, 1957, 1960, 1968, 1981). Koteswaram (1958), in his pioneering paper on the easterly jet stream in the tropics, concluded that the greatly elevated surface of the vast Tibetan Plateau serves to heat directly the middle troposphere and to produce a strong solenoid field in the upper troposphere.

Our knowledge of the 'Tibetan anticyclone (or south Asian High)' was greatly enhanced by Krishnamurti's analysis of the, 200-hPa streamline charts based on his extensive collection of commercial aircraft data (Krishnamurti and Rodgers, 1970; Krishnamurti, 1971a,b). A word of caution is needed here, however. The Tibetan anticyclone is not a purely thermally driven system maintained on the Plateau. As Krishnamurti (1985) has demonstrated, its center is located over the western tropical Pacific during northern winter and moves over south-east Asia in May. In their recent studies, Wu and his colleagues (Liu *et al*., 2001; Zhang *et al*., 2002; Wu and Liu, 2003) refer the term 'south Asian High (SAH)' only to the huge upper tropospheric anticyclone that appears over south Asia in the summer half year, and showed that the SAH possesses bimodality that is composed of the Tibetan mode and the Iran mode, with each corresponding to distinct climate anomaly patterns.

13.1.3 Early progress of Tibetan Plateau research in China

The systematic research of Tibetan Plateau meteorology in China started from 1950. On analysing the upper tropospheric circulation over Asia in the winter from 1945 to 1946, Yeh (1950) found that due to the Tibetan Plateau forcing, the westerly jet is split into two branches with the south branch established in mid-October, and the downstream trough becoming strongly tilting from the north-east to south-west. This is in good accordance with the theoretical results of Bolin (1950). Koo (1951) further emphasizes such a splitting impact of the Tibetan Plateau, and showed that downstream of the Plateau, the north and south branches of the westerly merge into one jet stream, which becomes the strongest in the World. In 1951 in a study of the onset and retreat of the jet stream over Asia, Yeh *et al*. (1951) already noticed the 'abrupt seasonal change' of circulation over Asia in 1945–1946. Yeh (1952) also pointed out that the influence of the Tibetan Plateau on the atmosphere depends

on the circulation patterns it encounters, and varies from one season to another. At the same time, Chu (1957a,b) used a two-layer numerical model to simulate the impacts on stationary waves of large-scale heating sources/sinks and orography, and found that both the Tibetan Plateau and Rockies can generate the ridge/trough pattern along the westerlies reasonably well. Cao (1957) treated the impacts of the Tibetan Plateau and Rockies as the lower boundary conditions of an atmospheric dynamic system and obtained similar conclusions in his analytical solutions. Together with many other studies, the early research on the dynamical impacts of the Plateau on general circulation by Yeh and his colleagues led to the establishment of the meteorology of the Tibetan Plateau in the 1950s.

In 1957, Yeh and his colleagues published a paper entitled 'the wind structure and heat balance in the lower troposphere over the Tibetan Plateau and its surrounding' to show the wind field and heat balance in the lower troposphere over the Plateau. They found that in winter the westerlies are split to the west of the Plateau but converge to its east; whereas in summer the wind field is featured by a cyclonic circulation in the lower layer, which turns to anticyclonic at high levels. In winter most of the Plateau region is dominated by a descending motion except its south-eastern part, whereas in summer ascending motion prevails. More importantly they used for the first time the air–ground temperature difference, instead of the air temperature itself, to study the thermal status of the Tibetan Plateau in different seasons and revealed the fact that in summer the Plateau is a thermal source and in winter is a thermal sink, except for its south-eastern part. This study was followed by the classic 3-part paper by 'Staff Members of Academia Sinica' (1957, 1958a,b, with Yeh as the principle author) published in *Tellus*. In Part II of this paper, the influence of the Tibetan Plateau on the circulation over Asia was discussed dynamically, and a brief discussion of 'likely' heat sources in summer and heat sinks in winter were inferred. As evidence, the observed 'plateau-scale' diurnal variation was illustrated. In Part III, influence of topography on the general circulation was discussed using the quasigeostrophic vorticity equation with orographic forcing. In the *Rossby Memorial Volume*, Yeh *et al.* (1959) emphasized the global nature of the abrupt change of the upper air circulation in the northern hemisphere in June and October. They also discussed the changes in relation to the south-west monsoon in India and of Meiyu in China and Japan.

Since then, efforts have been made to find the thermal state of the Tibetan Plateau and to understand how such an elevated heating source and sink affect the local and global weather and climate. Ye *et al.* (1974) found that in the summer half year, the convective activities over the Plateau are well developed, and the non-linear interaction between large-scale systems and small-scale systems are important for maintaining the aforementioned summertime circulation patterns over the Plateau. Chen (1964) and Ye *et al.* (1979b,c,d, 1981) showed that strong ascending air over the Plateau flows eastward along the westerlies in the upper troposphere toward the eastern Pacific and North America. In summertime, the ascending air flows westward along the easterlies then subsides over Iran and other middle Asia regions, resulting in a dry climate. They also showed that in the meridional direction the summertime Tibetan Plateau ascending air subsides in

mid-latitudes to its north and in the southern hemisphere to its south, influencing the climate in these areas.

During the last 30 years, annular experiments, numerical modeling, and field experiments have been employed to investigate the climate impacts of the Tibetan Plateau. Based on various annulus experiments, Ye and Chang (1974), Chang *et al.* (1977), and Yang (1980) demonstrated that the Plateau not only split the westerlies into north and south branches, but also changed the propagation speed of large-scale waves along the westerlies in winter months. In summer, weak heating of the Plateau with strong background westerlies only affect the intensity of stationary waves, whereas strong heating over the Plateau contributes to the establishment of the Tibetan High, and weak westerlies can generate vortices on the eastern flank of the Plateau under its mechanical and thermal perturbation (Li *et al.*, 1976). Their experimental results also implied that the strong heating over the Tibetan Plateau in summer produces a super moist adiabatic lapse rate near the surface. This, together with strong lower layer convergence, leads to the general development of convections over the Plateau in summer.

It is clear from the description made above, the Tibetan Plateau has been considered important for both its dynamical and thermal impact on the large-scale circulation by keen analysis of upper level charts and by theoretical consideration. The subsequent work by Chinese meteorologists before the First GARP Global Experiment (FGGE) (including preliminary work on heat budgets and laboratory experiments) were summarized by Ye and Gao (1979b) in *Meteorology of the Tibetan Plateau.*

13.2 LARGE-SCALE FEATURES OF THE ATMOSPHERE NEAR THE TIBETAN PLATEAU

13.2.1 Large-scale flow and temperature fields

The stream fields at the upper, middle, and lower tropospheric levels for January (left) and July (right) are shown in Figure 13.2. The data are from the National Centers for Environment Prediction/National Center for Atmospheric Research (NCEP/NCAR) reanalysis (Kalnay *et al.*, 1996) from 1958–1997. The most striking feature of the stream field at 1,000 hPa in January is the divergence of air flow from the Tibetan Plateau to the surrounding areas, in particular to the southern hemisphere over the Indian and western Pacific Oceans. In July, although the pattern of stream field at 1,000 hPa looks similar to its wintertime counterpart in general, the directions of flow around the Tibetan Plateau are completely reversed. This implies the important impacts on the atmospheric circulation of the land–sea heating contrast (Chou, 2003) and the Tibetan Plateau (e.g., Tang and Reiter, 1984; Hsu *et al.*, 1999). Air converges toward the Tibetan Plateau from the surrounding areas, particularly from the southern hemisphere. The reversal of wind directions over the Arabian Sea and India, the eastern Bay of Bengal (BOB) and western Indo-China peninsula, South China Sea (SCS), and the western Pacific corresponds, respectively,

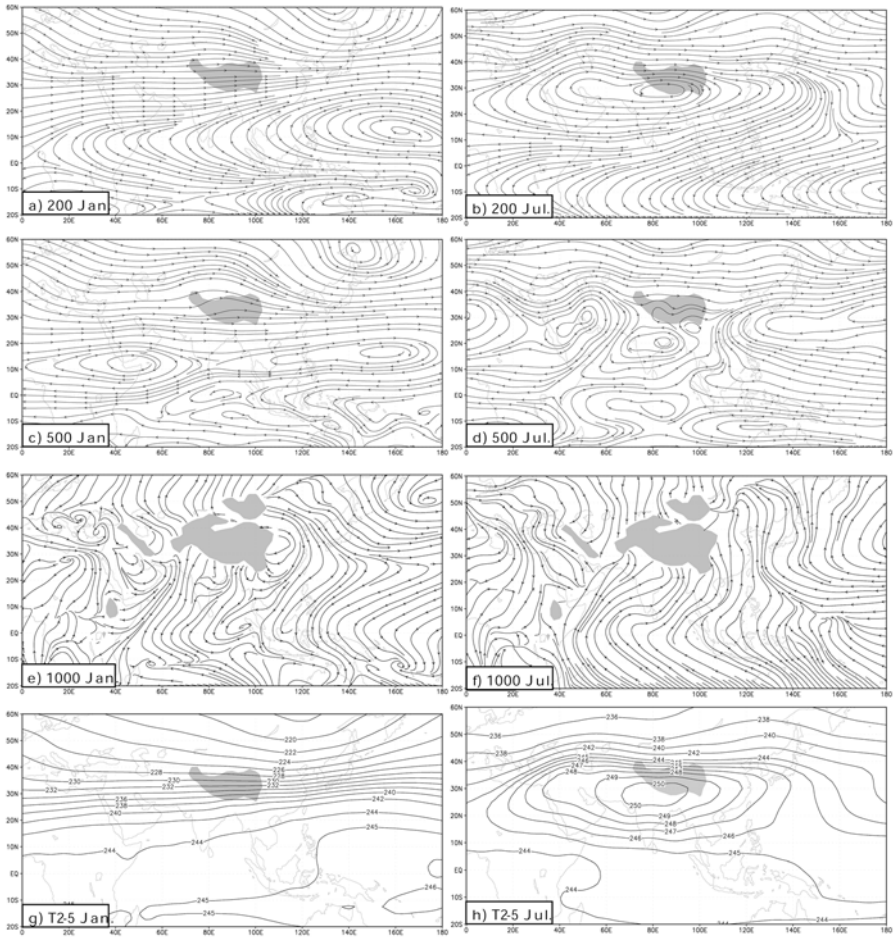

Figure 13.2. January (*left*) and July (*right*) mean stream fields at 200 hPa ((a) and (b)), 500 hPa ((c) and (d)), and 1,000 hPa ((e) and (f)) and the mean temperature fields averaged from 200–500 hPa ((g) and (h)) based on the NCEP/NCAR reanalysis and averaged over the period from 1958 to 1997.

to the south Asian, BOB, SCS, and western Pacific monsoons (e.g., Wu and Zhang, 1998; Ueda and Yasunari, 1998; Wang and Lin, 2002).

At 500 hPa, the mechanical influence of the Tibetan Plateau on the impinging westerlies in January is evident, although not as prominent as at 700 hPa (figure not shown), and most part of the Plateau is controlled by a high ridge. This then contributes to the formation of the wintertime semipermanent planetary-scale ridge between 40° and 120°E in high latitudes. In July, the anticyclone belt that goes around the subtropics in the northern hemisphere is broken over the Tibetan Plateau domain. A strong cutoff cyclone exists to its south and over the North

Indian Ocean, India, and the Indo-China Peninsula area. These are associated with the Tibetan Plateau heating and the Asian monsoon as will be discussed later.

At 200 hPa in January, a strong east Asian trough in the north and a huge subtropical anticyclone in the south dominate the north-western Pacific, forming a 'wind tunnel' along the subtropics. Westerly jets initiate from the Mediterranean Sea, penetrate the Asian subtropics, and merge into the tunnel, forming the strong east Asian jet. By July, the westerly jet retreats northward to high latitudes. In the subtropics, although a tropical upper troposheric trough is located over the North Pacific, a huge anticyclone is observed over the entire Afro-Asian continental area. This upper tropospheric continental anticyclone exists only in the summer half year, and is usually named as the Tibetan or south Asian High (SAH). It differs in nature from the aforementioned upper tropospheric anticyclone over the western Pacific in the winter half year (e.g., Krishnamurti, 1985). As reported by many studies (e.g., Flohn, 1957, 1960; Mason and Anderson, 1963; Tao and Zhu, 1964; Krishnamurti, 1971a,b; Krishnamurti *et al.*, 1973b; Luo *et al.*, 1982; Wang, 1987; Zhang *et al.*, 2002), the formation of the SAH is associated with the strong summertime continental heating and the latent heat release associated with the Asian monsoon. Based on the NCEP/NCAR reanalysis, Wu and Liu Y. (2003) and Liu Y. *et al.* (2004) found that the subtropical anticyclonic circulation exists over each of the continents in summer mainly due to the summertime continental heating. The SAH becomes the strongest because of the larger scale of the Eurasia continent, the existence of the Tibetan Plateau, and the strong latent heat release associated with the east Asian monsoon (Wu *et al.*, 1999; Liu Y. *et al.*, 1999, 2001). On the other hand, the formation of the upper tropospheric anticyclone over the western Pacific in winter is in association with the warm sea surface temperature (SST) of the warm pool in the western Pacific. Deep convections are widespread over this area, and their latent heat release contributes greatly to the formation of the upper tropospheric anticyclone.

The mean upper tropospheric temperature averaged from 200 to 500 hPa for January and July are shown, respectively, in Figure 13.2(g) and (h). In January (Figure 13.2(g)), the area warmer than 246 K is over the western equatorial Pacific, and the cold trough is over the eastern Siberia in high latitudes. A baroclinic belt with strong meridional temperature gradient along the subtropics is then intensified over east Asia just between the warmest center to the south and the coldest center to the north. These are in good coordination with the wintertime 200-hPa geopotential configuration as demonstrated in Figure 13.2(a) (i.e., a strong westerly jet stream, which is intensified over east Asia, is sandwiched by an anticyclone to the south and a trough to the north). In July, the warmest center of over 250 K is observed to the south of the Tibetan Plateau where the maximum summer monsoon rainfall occurs. It is also in good coordination with the center of the huge SAH as demonstrated in Figure 13.2(b).

The circulation features around the Tibetan Plateau, as presented in Figure 13.2, are closely related to the Tibetan Plateau forcing. Figure 13.3 shows cross sections along 30°N and 90°E of the January (a and b) and July (c and d) mean potential temperature and wind vector projected on the corresponding cross sections in which

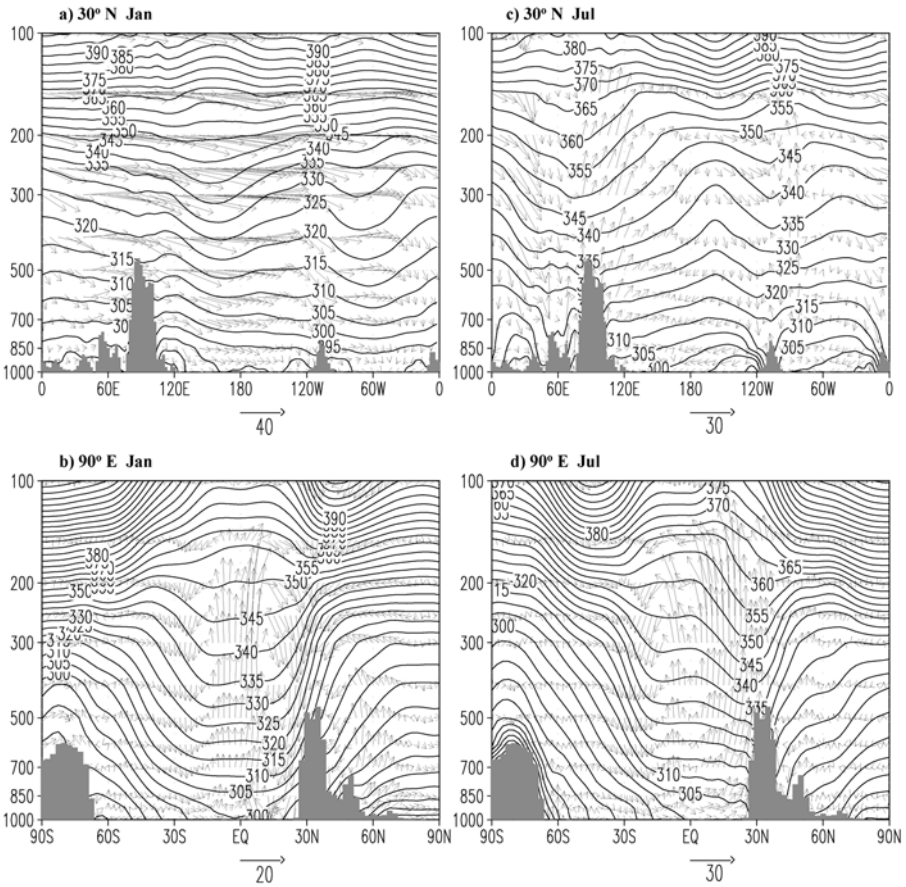

Figure 13.3. January (*left*) and July (*right*) mean (1986–1995) cross sections of potential temperature (contour interval: 10 K) and vertical circulation (vectors) along 30°N ((a) and (c)) and 90°E ((b) and (d)).

the vertical velocity w has been multiplied by 10^3. These cross sections are based on NCEP/NCAR reanalysis from 1986–1995. In January along 30°N, cold temperatures over continents and warm temperatures over oceans are prominent. Atmospheric cooling indicated by air descent ($\vec{V} \times \nabla\theta < 0$) prevails in the free troposphere. Along 90°E, the strongest cooling is over the Tibetan Plateau and to its south, whereas the strongest heating exist between 15°S and 10°N, corresponding to the intertropical convergence zone (ITCZ) rain belt with rainfall rate more than 4 mm per day (figure not shown). An enhanced local Hadley cell is therefore observed between 20°S and 30°N. During summer, the warmest center of potential temperature is just over the Tibetan Plateau. This is in agreement with the existence of the warm temperature center in July over the Plateau (Figure 13.2(h)). Strong ascent prevails in the area from the Tibetan Plateau to eastern China on the east and

to the BOB to the south, penetrating the isentropic surfaces almost perpendicularly and indicating the existence of a strong heating source over the area in summer (Kuo and Qian, 1981, 1982; Zheng and Liou, 1986; Liu X. *et al*., 2002; Wu, 2004). The cooling and descent of the air column over the Tibetan Plateau in winter accounts for the existence of surface divergence flow, whereas the heating and ascent of the air column over the Plateau in summer explains the existence of the surface flow convergence and accounts partly for the intensification of the SAH over the Plateau, as shown in Figure 13.2.

13.2.2 Mechanical effects of the Tibetan Plateau on large-scale motion

'The Tibetan Plateau is roughly of ellipsoidal shape with a major axis oriented in west–east direction. This will split the westerlies and force them to flow around it. The splitting of the westerlies is very pronounced on daily 500-mb charts. Due to the fact that in a rotating fluid the motion has a strong tendency to be quasi-2-D the splitting is also observed well high above the Plateau.' (Staff Members of Academia Sinica, 1958a.) This unique orographic influence of the Tibetan Plateau on the large-scale circulation has also been emphasized by Murakami (1981a,b, 1987).

Tokioka and Noda (1986) studied the effects of large-scale orography on January atmospheric circulation using a general circulation model (GCM). They performed four experiments under the perpetual January condition to isolate the orographic effects of the Tibetan Plateau and those of the Rockies and Greenland. They showed that the large-scale mountains tend to divert flows around the orography. The ascending (descending) center shifts poleward (equatorward) in the upwind (downwind) side of mountains. As for the zonal wavenumber 1, the surface vertical motions are very different from what are expected from the linear kinematical surface boundary condition (e.g., Charney and Eliassen, 1949).

Trenberth and Chen (1988) discussed the planetary-scale response of the atmosphere to the kinematic effects of orographic forcing by the Tibetan Plateau–Himalayan mountain complex. The key point of this analysis is to retain a term related to the perturbation in the horizontal motion in the kinematic lower boundary condition (LBC). From a scaling analysis they deduced a critical mountain height h_c beyond which the component of flow 'around' will dominate that 'over' the orography. The h_c is proportional to the meridional scale of the orography and depends on latitude. For a north–south scale appropriate for the Himalayan complex $h_c \sim 1.5$ km, which is much less than the actual height of the Plateau ($\sim$4 km), implying that the 'around' component will dominate. On the other hand, while the westerly flow impinges on a large-scale orography such as the Tibetan Plateau and goes around in the lower layers, the atmospheric westerly angular momentum is lost due to the reaction of the mountain. At the same time, the orography also plays an important role by drawing on the zonal mean kinetic energy and converting it into eddy kinetic energy. By considering the conservation constrains of both energy and angular momentum, Wu (1984) deduced a critical mountain height h_c as a function of the phase difference between the pressure perturbation and orography (λ_0) and the frictional coefficient (α):

$h_c = 8\sqrt{2}\alpha(3\sin\lambda_0)^{-1}$. Taking $\alpha = 230\,\text{m}$ and λ_0 from $\pi/2$ to $\pi/6$, h_c varies from 870 m to 1.5 km. When a mountain height is $h < h_c$, the climbing effect of the mountain is important, and the linear theory of planetary waves is acceptable. When $h > h_c$ the deflection effect becomes important, and the response of the atmosphere to the mountain forcing is non-linear.

In a following paper, Chen and Trenberth (1988a) studied the orographically forced planetary waves in the northern hemisphere winter, using a linear steady-state model with the wave-coupled lower boundary formulation. They demonstrated that the wave-coupled LBC has significant impact on the forced planetary waves. The most noticeable difference in response of the planetary wave appears near the Himalayas. The wave-coupled LBC allows the total flow at the lower boundary to circumvent the Himalayas, unlike the traditional LBC. The kinematic effects of the Himalayas alone form the basis for a quite realistic Siberian High and Aleutian Low, and the resulting east Asian trough is close to the observed position. In Cheng and Trenberth (1988b) they included thermal forcing in the model. When both orographic and thermal forcings are included, the simulation produces excellent results which are compared in detail with observations.

13.2.3 Winter cold surge and the role of the Tibetan Plateau

During winter, the thermal effect becomes less important than the mechanical effect of the Tibetan Plateau. The low-level westerlies split into two main streams that flow around the Plateau. A phenomenon unique to the east of the Tibetan Plateau is the frequent occurrence of low-level cold surges bursting out of Siberia and reaching as far south as the South China Sea and even Indonesia (e.g., Boyle and Chen, 1987; Murakami, 1981b, 1987).

The generation mechanisms of the cold surges were investigated by Nakamura and Murakami (1983) and by Murakami and Nakamura (1983), using a ten-layer hemispheric model. Since the thermal effect is not significant during winter, the diabatic heat source is simplified to the form of Newtonian cooling. A hypothetical Tibetan Plateau was prescribed to be elliptic (40 degrees in longitude and 30 degrees in latitude) and Gaussian-shaped in the vertical with a maximum height of 5 km. They confirmed that the orography of the Tibetan Plateau has a dominant effect on lee cyclogenesis and associated northerly surges. These phenomena were preceded by the development of a small-scale edge anticyclone trapped in a shallow layer near the north-east corner of the Plateau. Nakamura and Doutani (1985) extended the work and examined the detailed structure of the edge front associated with the cold surge, using a higher resolution model with a 1×1 degree horizontal grid interval and 16 vertical levels. A strong cold front was formed at the north-east corner of the elliptic-shaped model mountain. The ageostrophic northerly wind with a magnitude of 20 to $25\,\text{m s}^{-1}$ appeared across the cold front. This edge front was trapped along the mountain boundary and propagated clockwise with a speed of 20 to $25\,\text{m s}^{-1}$. This behavior indicates the similarity between edge waves and coastal Kelvin waves.

Sumi (1985) investigated cold surges around the Tibetan Plateau obtained in a numerical prediction model. Cold surges trapped in the periphery of the mountain

and in the lower troposphere were well simulated in the model. To investigate the mechanism of cold surges, momentum budget analyses at the 850-mb level were performed on two cases showing increases in northerly winds. Initially, an increase of the northerly wind was associated with the southward passage of a cold front. However, this northerly wind weakened gradually at the south-eastern corner of the Tibetan Plateau. The major increase of the northerly wind occurred in the cold air behind the cold front and was propagated further southward. Although the effect of the ageostrophic component played a dominant role in the early stage of propagation, the effect of the non-linear advection term became important in the late stage. Because of this effect, the northerly wind left the mountain and traveled farther southward. Sumi and Toyota (1988) made a detailed observational study of the edge disturbances around the Tibetan Plateau which were found in the numerical simulations. Two types of orographic effects are found: one is the effect upon synoptic disturbances, which corresponds to the main cold surge events; and the other is the excitation of the edge disturbances. A relationship between the intensity of a trough ahead of the Plateau and the excitation of edge disturbances is suggested.

Lu and Zhu (1991) developed a theory in terms of the linear shallow-water wave equation involving a huge topographic effect. Two kinds of gravitational wave solutions are derived with the assumption that the plateau in question is a vast topography, inclined at a constant slope from west to east. One set of solutions corresponds to two high-frequency inertia–gravitational waves, another solution is one of a low-frequency, orographic gravitational wave excited by the huge topography. The latter is similar to Kelvin waves in some respects. The path of gravitational wave rays is described by a hypocycloid equation. The result agrees quite well with the fact that the center of the cold surge strong wind moves in a curved path along the eastern fringe of the Tibetan Plateau.

13.2.4 Summertime negative vorticity source over the Tibetan Plateau

Figure 13.4 shows the July mean cross sections of geopotential height deviation from the corresponding zonal means (a) along 30°N and (b) along 90°E. A unique feature over the Tibetan Plateau is clearly seen: in summer, there is a strong but very shallow lower tropospheric low underlying a strong and deep high in the upper troposphere. The maintenance mechanism concerning such a peculiar large-scale circulation feature has attracted continuous efforts (Yeh, 1950; Yeh *et al.*, 1957; Ye and Gao, 1979b; Luo and Yanai, 1984; Yanai *et al.*, 1992; Yang *et al.*, 1992; Ye and Wu, 1998). In this section, the theory of Ertel potential vorticity is employed to provide new insights into the problem (Wu *et al.*, 2004).

As demonstrated in Figure 13.3, in the boreal summer the isentropic surfaces between 315 to 335 K intersect with the Tibetan Plateau while remaining continuous surfaces over the other parts of the World. A study by Haynes and McIntyre (1987) has shown that there is no net creation and destruction of potential vorticity between two complete isentropic surfaces. The intersection of those isentropic surfaces with the plateau as shown in Figure 13.3 then suggests that *the Tibetan Plateau is an*

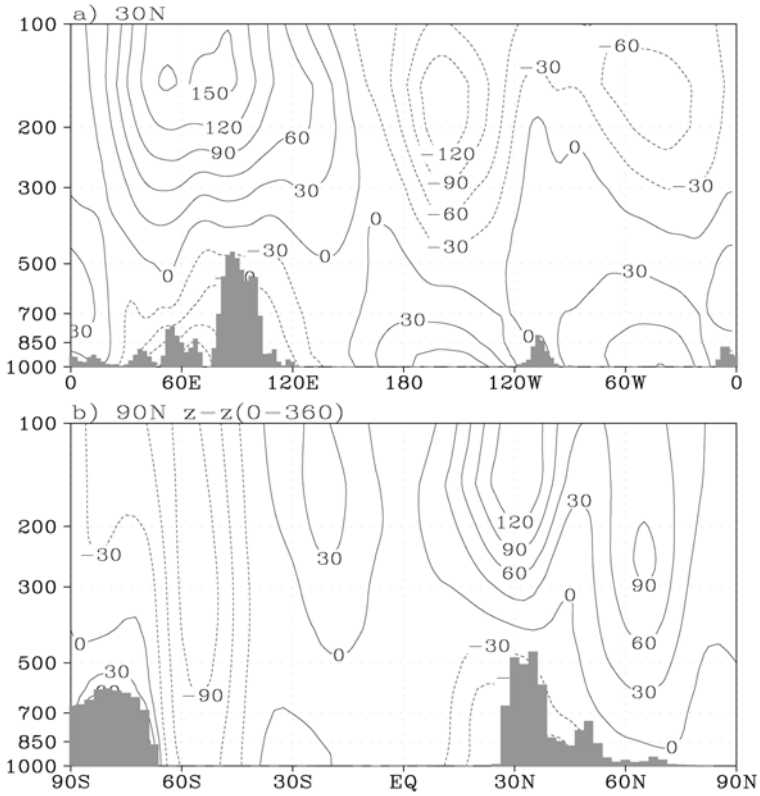

Figure 13.4. 1980–1997 July mean cross sections of geopotential height deviation from the corresponding zonal mean (a) along 30°N and (b) along 90°E (in units of geopotential meter (gpm)).

important source of potential vorticity for atmospheric motions in summer. The land surface sensible flux over the Tibetan Plateau in summer can be more than $100\,\mathrm{Wm}^{-2}$. This heat source is transferred to the atmospheric column by diffusion and produces a maximum heating of about $10\,\mathrm{Kd}^{-1}$ near the surface. Since the diffusive sensible heating is very strong near the surface and decreases gradually with increasing height, the atmospheric thermal adaptation (Hoskins, 1991; Wu and Liu, 2000) to such a heating should produce cyclonic vorticity in a shallow lower layer, but negative vorticity in the deep upper layers aloft. Therefore, it would be instructive to employ the flux form of the Ertel potential vorticity equation (Ertel, 1942) to gain new insights on the maintenance of the circulation pattern shown in Figure 13.4. For this purpose, Liu *et al.* (2001) and Wu *et al.* (2004) took the monthly average of the equation:

$$\frac{DW}{Dt} = \frac{\partial W}{\partial t} + \nabla \times (\vec{V} W) = \vec{F}_\zeta \times \nabla\theta + \vec{\zeta}_a \times \nabla Q \tag{13.1}$$

where $Q(=\dot{\theta})$ denotes diabatic heating; $\vec{\zeta}_a$ the 3-D absolute vorticity; $\vec{F}_\zeta$ the frictional dissipation rate of $\vec{\zeta}_a$; ∇ the 3-D Hamilton operator; and

$$W = \rho P = \vec{\zeta}_a \times \nabla\theta \tag{13.2}$$

is the amount of Ertel potential vorticity (P) per unit volume (Haynes and McIntyre, 1987). Liu *et al.* (2001) and Wu *et al.* (2004) then performed diagnosis by using the 12-hour (00Z and 12Z) NCEP/NCAR reanalysis data for July from 1986 to 1995. In such circumstances, the local time change is small and can be omitted. Let the overbars indicate the monthly mean and the primes indicate the deviation from it. Equation (13.1) can then be written as:

$$\nabla \times \bar{\vec{V}}\bar{W} = \bar{\vec{\zeta}}_a \times \nabla\bar{\dot{\theta}} + R \tag{13.3}$$

where the term on the left denotes the divergence of the potential vorticity flux; the first term on the right is the generation of potential vorticity due to diabatic heating; and

$$R = \overline{\vec{\mathbf{F}}_\zeta \times \nabla\theta} + \overline{\vec{\zeta}_a' \times \nabla\dot{\theta}'} - \nabla \times \overline{\vec{\mathbf{V}}' W'} \tag{13.4}$$

is the residual which represents the effects of frictional dissipation and transient processes with timescales of less than 12 hours. Since transient heating data are absent from the reanalysis, the diabatic heating rate ($\dot{\theta} = d\theta/dt$) is inversely computed from the distribution of θ at each time step, and R is calculated as the difference between the two other terms in (13.3). The σ coordinate system is used in the calculation. The two levels of $\sigma = 0.435\,7$ and $\sigma = 0.995$ are chosen to represent the upper and lower layers of the atmosphere. The former is near 250 hPa and the latter is near the ground over the Tibetan Plateau. Due to the large diurnal variation in diabatic heating over the Plateau (Ye and Gao, 1979b; Yanai *et al.*, 1992), the usage of the 12-hour analysis may present a sampling problem in calculating the magnitudes of those terms contained in (13.3) and (13.4). However, this will not affect the qualitative evaluation of the potential vorticity balance from (13.3).

The potential vorticity (PV) budget at $\sigma = 0.435\,7$ is shown in Figure 13.5(a) and (b). The distribution of the divergence of the PV flux (Figure 13.5(a)) exhibits two strong negative centers with intensities of more than $2 \times 10^{-12}\,\mathrm{Km^{-1}\,s^{-2}}$ on the eastern and north-western flanks of the Tibetan Plateau. They are in good agreement with the distribution of the generation of negative PV (Figure 13.5(b)) that is due to the decrease with height of diabatic heating. Thus, we can infer that the effects of the frictional dissipation and the transient processes are small in the upper troposphere, although cumulus friction can exist when cumulus convection is active (e.g., Tung and Yanai, 2002). It is somewhat strange that in Figure 13.5(b) no center exists over the heavy rain regions such as at the head of the BOB and southern China. One possible explanation is that over these regions the $\sigma = 0.435\,7$ surface is just close to the level of maximum rainfall so that $\partial\bar{\dot{\theta}}/\partial z$ becomes small.

The PV budget at the $\sigma = 0.995$ level is shown in Figure 13.5(c–e). The strong center of positive potential vorticity generation is due to the increase of diabatic heating with height on the southern side of the Tibetan Plateau, from 25°N to 31°N

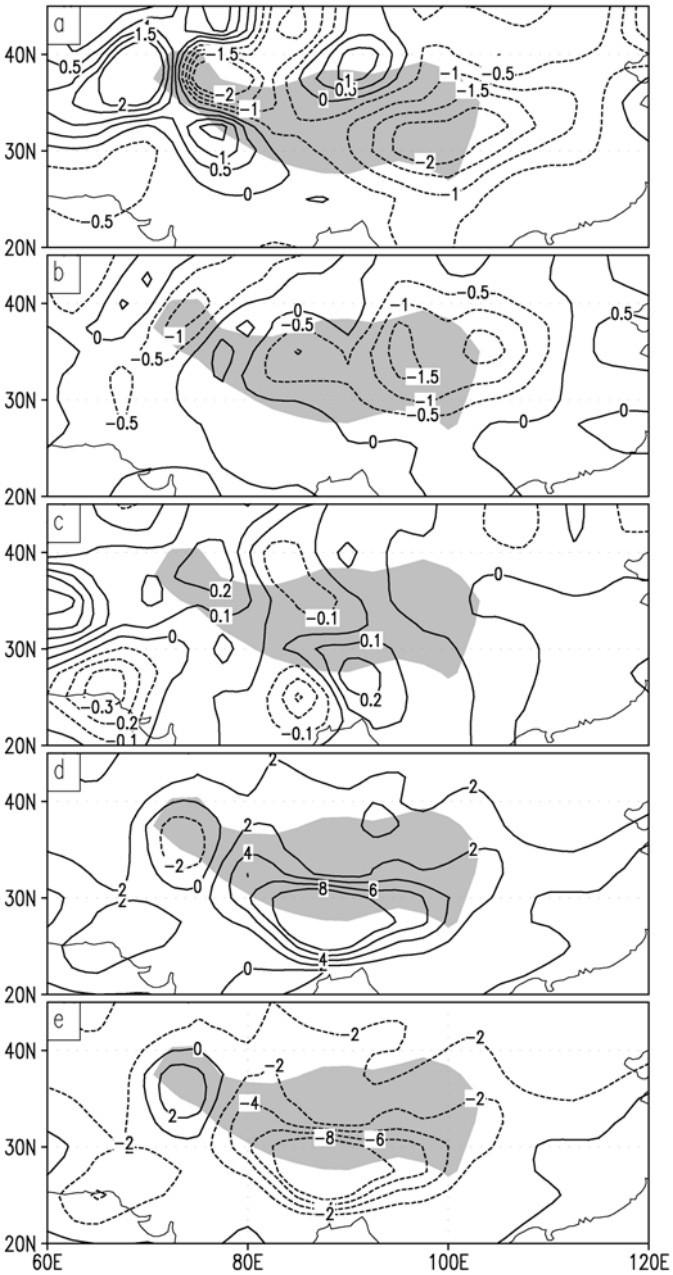

Figure 13.5. The July mean (1986–1995) PV budget calculated from the PV equation (13.3) at the $\sigma = 0.4357$ level ((a) and (b)) and at the $\sigma = 0.995$ level ((c), (d), and (e)). Regions higher than 3,000 m above sea level are shaded. Panels (a) and (c) are the divergence of the W flux; (b) and (d) are the generation of W due to diabatic heating; and (e) is the residual term R. The units are $10^{-12}\,\mathrm{Km}^{-1}\,\mathrm{s}^{-2}$.

(Figure 13.5(d)), revealing the importance of near-surface sensible heating in the maintenance of the lower layer cyclone over the Tibetan Plateau. On the other hand, the divergence of vorticity flux (Figure 13.5(c)) is too small to balance the vorticity generation. The heating term must be balanced mainly due to the frictional and transient processes (Figure 13.5(e)). The results obtained from the above analysis not only confirm the thermal adaptation theory, but also provide an interpretation for the formation of the atmospheric circulation over the Tibetan Plateau. It is mainly due to the strong surface sensible heating over the plateau that the shallow and strong surface cyclone and deep anticyclone aloft are maintained.

Further diagnosis of the cross-boundary flux of vorticity shows that the Tibetan Plateau area is a negative vorticity source in summer, and the negative vorticity is transferred outwards through its northern and eastern boundaries (Liu Xin *et al.*, 2001), affecting the circulation anomalies in the northern hemisphere. This will be discussed further in Section 13.4.

13.3 HEAT SOURCES ON THE TIBETAN PLATEAU

13.3.1 Various estimates of heating over the Tibetan Plateau

Ye and Gao (1979b) showed the monthly mean values of net heating of the air column of a unit cross section $\langle Q_1 \rangle$ (in notation used by Yanai *et al.*, 1973):

$$\langle Q_1 \rangle = \langle Q_{SR} \rangle + LR_1 - LR_2 + S + LP \tag{13.5}$$

where $\langle Q_{SR} \rangle$ is the absorption of solar radiation by the air column; LR_1 is the effective long-wave radiation from the ground surface; LR_2 the outgoing long-wave radiation at the tropopause; S the sensible heat flux at the surface; P the precipitation rate; and L the latent heat of condensation, for the western and eastern Plateau separately. In the western Plateau, the sensible heat flux dominates, and in the eastern Plateau the condensation heating becomes dominant after the onset of summer rains. These general features have not changed during the large numbers of subsequent studies.

Since the FGGE (December 1978–November 1979), renewed attempts have been made to examine the heat sources over the Tibetan Plateau and surrounding areas. Parallel with the FGGE, Chinese scientists conducted the Qinghai–Xizang Plateau Meteorology Experiment (QXPMEX) from May to August 1979. During QXPMEX, temporary surface, upper air, and radiation stations were added to the previously data-void region of the western and central Tibetan Plateau (see e.g., Shen, *et al.*, 1984; Liou and Zhou, 1987; Zhang *et al.*, 1988; Yanai and Li, 1994).

Yanai *et al.* (1992) tabulated 16 papers on the Tibetan heat sources published since 1979, according to the type of method used.

(1) Method A (Q_1: *apparent heat source*, and Q_2: *apparent moisture sink* as residuals of the large-scale atmospheric heat and moisture budgets, following Yanai *et al.*

(1973)). We can show that the vertically integrated Q_1 and Q_2 satisfy:

$$\langle Q_1 \rangle = \langle Q_R \rangle + LP + S \ldots \tag{13.6}$$

and

$$\langle Q_2 \rangle = L(P - E) \ldots \tag{13.7}$$

where Q_R is the radiative heating rate; and E the rate of evaporation at the surface.

(2) Method B (surface and radiation measurements using (13.5) (e.g., Ye and Gao (1979b)).
(3) Method C (surface energy balance: estimates of $S + LE$ only).

Nitta (1983) was the first to use Method A to discuss the heating profiles over the Tibetan Plateau. Using the FGGE station data, he obtained the mean vertical profiles of the tropospheric heat source Q_1 and moisture sink Q_2 over several parts of the eastern Tibetan Plateau for a 100-day period from the end of May to early September 1979. He found that, over the eastern Plateau, heating occurs in a deep tropospheric layer and that the sensible heat flux from the surface and the release of latent heat of condensation contributes nearly equally to the total heating in this period.

Luo and Yanai (1983), using an objectively analyzed FGGE data set, studied the time evolution of the large-scale precipitation, low-level (850-hPa) wind, moisture and vertical motion fields, and horizontal moisture transport over the Tibetan Plateau and the surrounding areas during a 40-day period (26 May–4 July 1979) which included the onset of the Indian summer monsoon. They showed that the mean 850-hPa wind field exhibits a pronounced inflow toward the Plateau with diurnally varying intensity, confirming the earlier finding of Yeh *et al.* (1957) (also see Staff Members, 1958a,b). Subsequently, Luo and Yanai (1984) examined the large-scale heat and moisture budgets of the Plateau region during the 40-day period. They found that there is a deep heating layer over the Plateau and the mean heating rate in the 200–500 hPa layer above the Plateau is as intense as that over the Assam–Bengal region. They identified the principal components of the heat source as the sensible heat flux from the ground surface and the additional condensation heat from the summer rains, supporting the classical studies of Flohn (1968) and Ye and Gao (1979). They also showed that a deep, nearly mixed layer with high potential temperature is observed over the Plateau in the evening (1200 UTC) (upper level soundings were available only at 0000 and 1200 UTC). The mixed layer was especially pronounced during the dry preonset period.

He *et al.* (1987) extended the heat and moisture budget analysis to an 80-day period (16 April–4 July 1979) and over a larger domain (0–50°N, 40–130°E). They showed that, from spring to summer 1979, the general circulation over south Asia underwent two distinct stages of abrupt transitions, resulting in the successive onsets of the south-east Asian and Indian monsoons (e.g., Krishnamurti, 1985). The two onsets were related to a similar two stages of upper tropospheric warming over the Asian land mass. The rapid warming occurred first over longitudes east of

85°E (the eastern Tibetan Plateau–south China), and then over longitudes west of 85°E (Iran–Afghanistan–western Plateau). The successive warming over these regions is the primary cause of the successive reversals of the meridional temperature gradient on the south sides of these regions. They also showed the presence of the large-scale vertical circulation that is thermally induced by the Tibetan Plateau. The existence of the Plateau-induced vertical circulation is also evident in the distribution of subsidence in the surrounding desert areas (see also Manabe and Broccoli, 1990). In a case study of the Asian summer monsoon onset in 1989 based on the European Centre for Medium-Range Weather Forecasts (ECMWF) analysis, Wu and Zhang (1998) obtained the similar result that before the monsoon onset, the upper tropospheric temperature over the eastern Plateau and along the Yangtze River is several degrees celsius warmer than over the western Plateau. They demonstrate that this is mainly due to the strong westerlies over the Tibetan Plateau before the monsoon onset, which advects cold air from the west to compensate the local heating of 2 to 4°C per day over the Plateau.

Using the FGGE and QXPMEX data, Yanai *et al.* (1992) further studied the seasonal changes in the large-scale circulation, thermal structure, and heat sources and moisture sinks over the Tibetan Plateau and the surrounding areas for a 9-month period from December 1978 to August 1979. They showed that the air above the Tibetan Plateau is warmer than the air over the surrounding areas when compared at the same level and the same latitude (Figure 13.2(h)). They also described the seasonal change of a large-scale vertical circulation that is thermally induced by the Plateau (Figure 13.3). In northern summer, this circulation merges with the circulation associated with the monsoon rain belt which has migrated from the Indian Ocean. Both the warm air and the vertical circulation over the Plateau exhibit pronounced diurnal variations. They also verified that the Plateau is a heat sink in winter and becomes a heat source in spring as shown previously by Ye and Gao (1979b).

Li and Yanai (1996) studied the onset and interannual variability of the Asian summer monsoon in relation to land–sea thermal contrast using a 14-year (1979–1992) set of the global analyses prepared by the ECMWF. The onset of the Asian summer monsoon is concurrent with the reversal of the meridional temperature gradient in the upper troposphere south of the Tibetan Plateau, as suggested by Flohn (1957). The reversal is the result of large temperature increases in May to June over Eurasia centered on the Plateau with no appreciable temperature change over the Indian Ocean (see Figure 13.10). In spring the Tibetan Plateau is a heat source that is distinctly separate from the heat source associated with the rain belt in the equatorial Indian Ocean (see Figures 13.9 and 13.10). The Tibetan heat source is mainly contributed to by the sensible heat flux from the ground surface, while the oceanic heat source is due to the release of the latent heat of condensation. It is the sensible heating over the Plateau region in spring that leads to the reversal of the meridional temperature gradient. Despite its intensity the condensational heating over the Indian Ocean does not result in tropospheric warming because it is offset by the adiabatic cooling of ascending air.

Recently, Ueda *et al*. (2003a,b) examined the heat source (Q_1) and moisture sink (Q_2) over the western and eastern Tibetan Plateau for a 4-month period from May to August 1998, using the Global Energy and Water Cycle Experiment (GEWEX) Asian Monsoon Experiment (GAME) 4-D data assimilation (4DDA) upper air data. In addition, they utilized the Climate Prediction Center Merged Analysis of Precipitation (CMAP) data (Xie and Arkin, 1997). They showed that there is substantial rainfall along the western and south-western slopes of the western Tibetan Plateau in May and June, contributing condensation heating to the western Plateau.

13.3.2 Heating over the Tibetan Plateau and the onset of Asian Monsoon

Here we show recent estimates of Q_1 and Q_2 using the 15-year (1979–1993) ECMWF reanalysis. This data set has been used in a study of the Australian summer monsoon (Hung and Yanai, 2004) and a study of the relationship between the Asian and Australian summer monsoons (Hung *et al*., 2004).

Figure 13.6 shows the horizontal distributions of the vertically integrated heat source $\langle Q_1 \rangle$ (top) and $\langle Q_2 \rangle$ (bottom) for December–February (DJF) and for June-August (JJA). In DJF, pronounced belts of heating exist along the southern side of the equator (South Africa, the South Indian Ocean, and the south-western Pacific) and off the east coast of Asia (Figure 13.6(a)). The essential nature of these heating belts becomes evident when we see the $\langle Q_2 \rangle$ field of the same season (Figure 13.6(c)). The south-of-equator heating belt is mainly due to condensation heating. On the other hand, over the region off east Asia, heating must come from sensible heating over the warm ocean, because $\langle Q_2 \rangle$ is negative, indicating that evaporation is exceeding precipitation.

During JJA, most of the major regions of heating including the two centers of heavy rain (the BOB–Bangladesh, and the western coast of the Indian subcontinent) associated with the Asian summer monsoon (positive $\langle Q_1 \rangle$ in Figure 13.6(b)) are also the regions of large moisture sink (positive $\langle Q_2 \rangle$ in Figure 13.6(d)). Exception is over the western Eurasian continent where $\langle Q_1 \rangle$ is positive but $\langle Q_2 \rangle$ is negative. A notable feature seen from Figure 13.6(b) and (d) is a well-known desert region of the Arabian peninsula where both $\langle Q_1 \rangle$ and $\langle Q_2 \rangle$ are negative, consistent with radiative cooling and evaporation exceeding precipitation in this region of subsidence.

In Figure 13.7 we show the annual cycles of the vertically integrated heat source $\langle Q_1 \rangle$ and moisture sink $\langle Q_2 \rangle$ for the western (top) and eastern (bottom) parts of the Tibetan Plateau separately. In this calculation, the Plateau (above 4,000 m) is divided into two parts (west of 90°E, and east of 90°E). The results for $\langle Q_1 \rangle$ for the two parts of the Plateau are qualitatively similar to those obtained by Ye and Gao (1979b) but the magnitudes are smaller than those given by Ye and Gao. For most of the year the Tibetan Plateau acts as a heat source. Only in winter months does the Plateau become a heat sink. Over the western Plateau, the sensible heat dominates except in July–September when the condensation heating becomes comparable and then dominant. In the eastern Plateau, the significance of condensation heating for May–October is evident. These results generally confirm the previous results (Nitta, 1983; Luo and Yanai, 1984; Yanai *et al*., 1992; Ueda *et al*., 2003b).

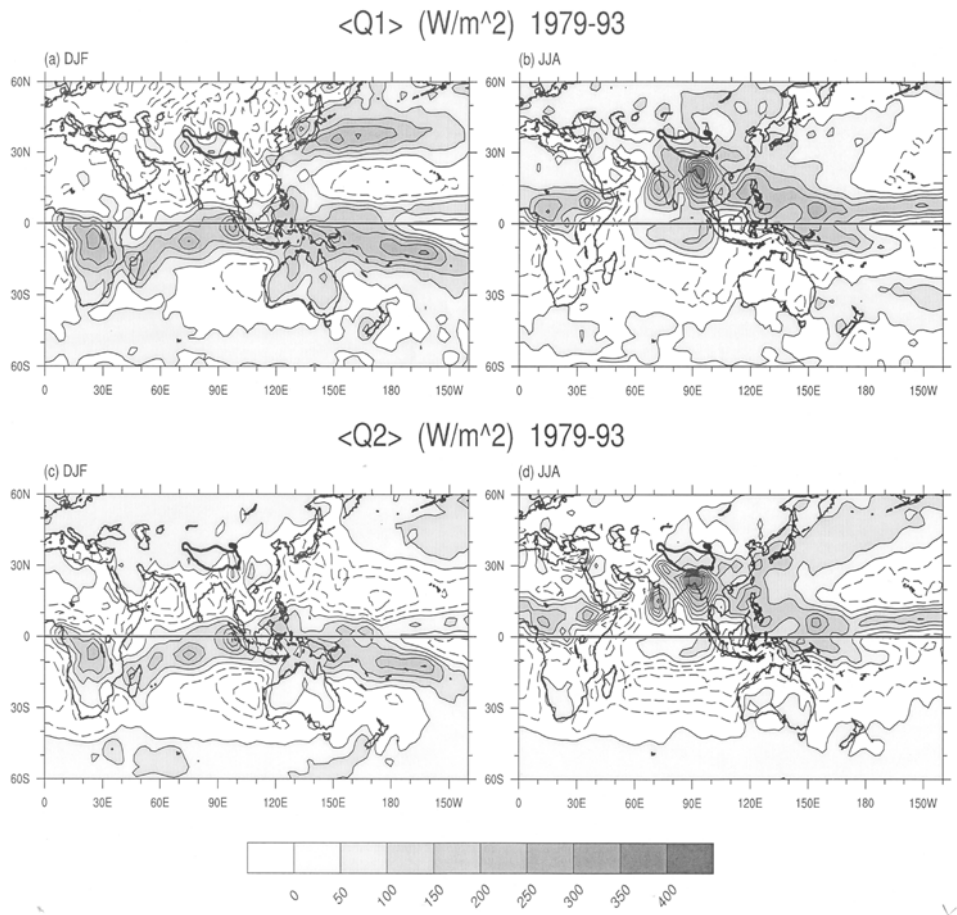

Figure 13.6. Vertically integrated heat source $\langle Q_1 \rangle$ (*top*) and moisture sink $\langle Q_2 \rangle$ (*bottom*), averaged for 1979–1993 for December–February (DJF) and June–August (JJA). (Units: $\mathrm{W\,m^{-2}}$.)

Figures 13.8(a) and (b) display the vertical–longitudinal distributions of Q_1 and Q_2 averaged between 27.5°N and 37.5°N in four seasons, respectively. There are three major regions of interest:

(a) The first is over the Tibetan Plateau. Figure 13.8(a) clearly indicates that there is a column of heating (positive Q_1) on the Plateau throughout the four seasons. But only in JJA and SON is the heating clearly related to Q_2 (condensation heating) of comparable magnitude. The lower half of the air above the Plateau is heated even in DJF and MAM, but there is very little contribution from Q_2, again suggesting the dominance of sensible heating in winter and spring.
(b) The mostly oceanic region east of the Tibetan Plateau is dominated by intense heating ($Q_1 > 0$). The strong heating in DJF just above the sea surface

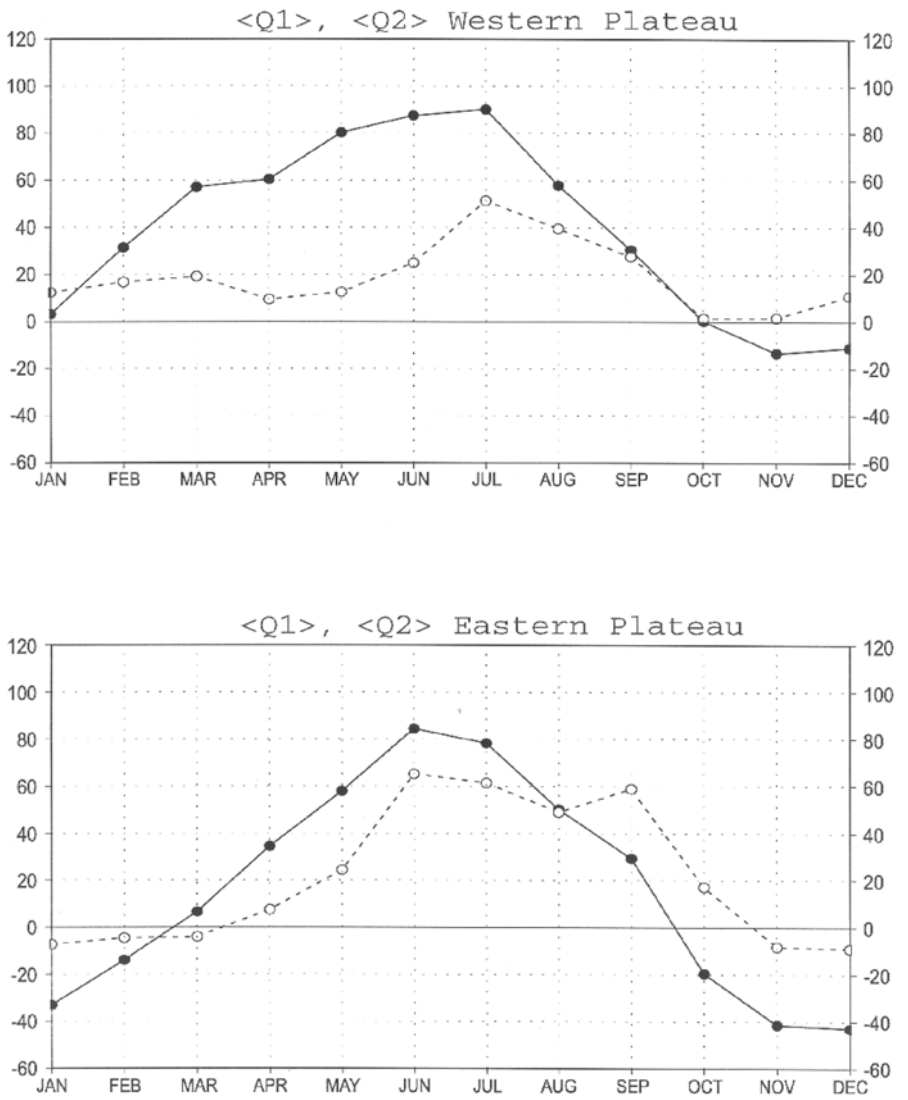

Figure 13.7. Annual cycles of the 1979–1993 mean vertically integrated heat source $\langle Q_1 \rangle$ (solid) and moisture sink $\langle Q_2 \rangle$ (dashed) over the western Tibetan Plateau (*top*) and over the eastern Tibetan Plateau (*bottom*). (Units: $\mathrm{W\,m^{-2}}$.)

(Figure 13.8(a), part (i)) is clearly related to the oceanic heat source off the east coast of Asia (Figure 13.6(a)). For the other three seasons, heating in this region is dominated by rain (Figure 13.8(b), parts (ii)–(iv)).

(c) The third region of interest is located to the west of the Tibetan Plateau. Especially during and after the monsoon season (JJA and SON), this region is

dominated by negative Q_1 and Q_2 (Figure 13.8(a), parts (iii–iv) and (b), parts (iii–iv)). As discussed by He *et al.* (1987) and Yanai *et al.* (1992), strong subsidence prevails in this region. Rodwell and Hoskins (1996) discussed the dynamics of desert formation in terms of a Rossby wave response to the monsoonal heating to the east.

Figure 13.9(a) and (b) display the vertical distributions of Q_1 and Q_2 averaged between 70°–100°E over four seasons, respectively. The large values of Q_1 and Q_2 seen near the equator are associated with the migrating ITCZ involving deep convection throughout the year. On the other hand, during spring (MAM), large values of Q_1 are seen from the surface to 250 hPa above the Tibetan Plateau (Figure 13.9(a), part (ii)). This heat source does not accompany Q_2 (Figure 13.9(b), part (ii)). This shows that the heating above the Tibetan Plateau in northern hemisphere spring is mainly contributed to by a sensible heat flux from the surface (e.g., Yanai *et al.*, 1992; Yanai and Li, 1994). After the onset of the Asian summer monsoon, heating from condensation in the ITCZ and heating over land merge together. In summer (JJA), large heating between surface and 200 hPa is centered over the southern edge of the Tibetan Plateau, although weak peaks of Q_1 and Q_2 are still observed between 10°S and the equator (Figures 13.9(a), part (iii) and 13.9(b), part (iii)).

Figure 13.10(a,b,c) shows the latitude–time sections of $\langle Q_1 \rangle$, $\langle Q_2 \rangle$ and the mean upper tropospheric (200–500 hPa) temperature averaged in the sector (70°–100°E) from 1979 to 1993. The daily $\langle Q_1 \rangle$ and $\langle Q_2 \rangle$ are averaged from the original 6-hourly estimates, and the upper tropospheric mean temperature is from ECMWF reanalysis. The thick curves in the figure indicate the solar declination angle.

We note a large region of positive values of $\langle Q_1 \rangle$ between 30° and 70°N from April to September in Figure 13.10(a) without corresponding features in $\langle Q_2 \rangle$ (Figure 13.10(b)). This region of positive $\langle Q_1 \rangle$ at high latitudes shows the sensible heating over the Asian continent including the Tibetan Plateau. On the other hand, large positive values in $\langle Q_1 \rangle$ between 20°S and 30°N are with large $\langle Q_2 \rangle$ and rainfall (not shown). A prominent rain belt is associated with the ITCZ moving between the two hemispheres (Figure 13.10(a) and (b)). During northern autumn (SON), the ITCZ propagates smoothly from north to south with some delay from the seasonal forcing. However, the ITCZ stays between 15°S–5°N from January to May without any north–south movement. Then, it shows a sudden northward jump in May–June at the onset of the Asian summer monsoon. The onset is concurrent with the reversal of the meridional temperature gradient in the upper troposphere over the BOB region (Flohn, 1957; Li and Yanai, 1996).

13.3.3 Mechanism of heating

Since Ye and Gao (1979b) it has been well recognized that the western and eastern Plateau have different heating characteristics (see Figure 13.7). For the western Plateau sensible heating dominates during spring, whereas for the eastern Plateau condensation heating dominates after the monsoon onset. This east–west contrast is related to the marked difference in the surface properties (e.g., Shi and Smith, 1992).

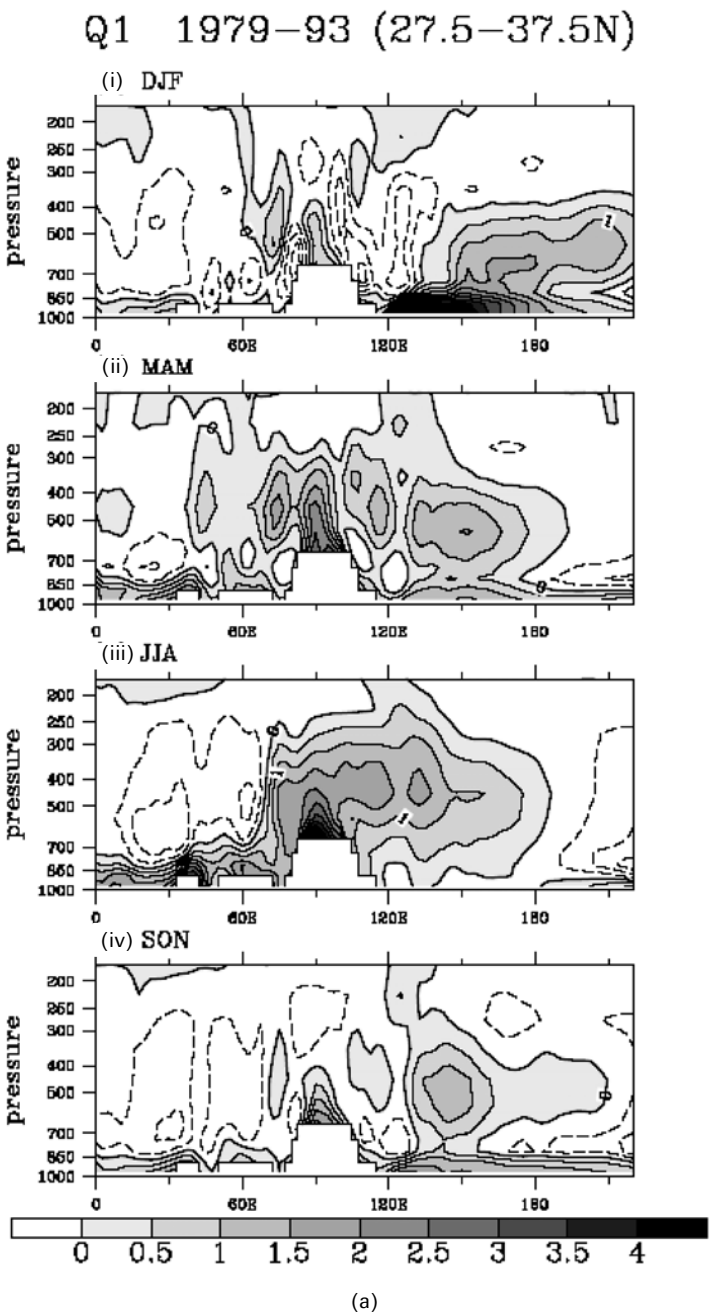

Figure 13.8. (a) Longitude–height sections of the 1979–1993 mean apparent heat source Q_1 for (i) DJF, (ii) MAM, (iii) JJA, and (iv) SON, averaged between 27.5°N and 37.5°N. (Expressed in units of K per day.) (b) Similar to (a), but for the 1979–1993 mean apparent moisture sink Q_2.

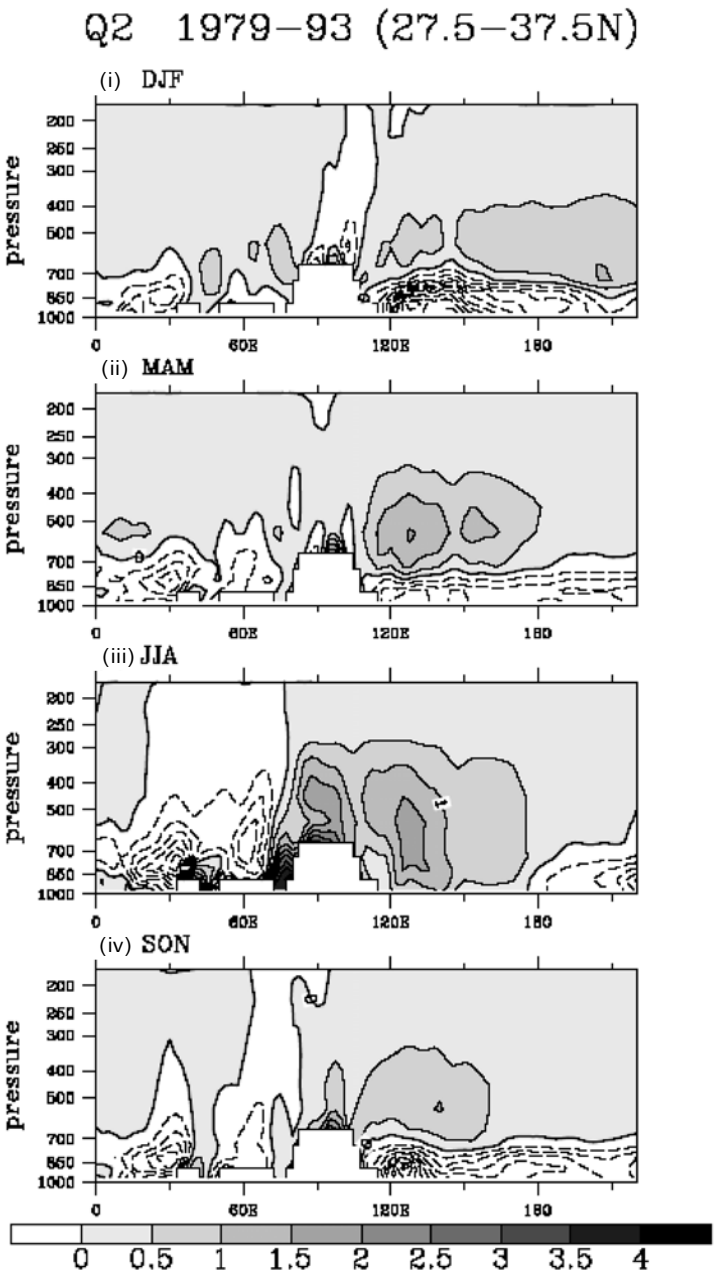
Q2 1979–93 (27.5–37.5N)
(i) DJF
(ii) MAM
(iii) JJA
(iv) SON
pressure
200
250
300
400
500
700
850
1000
0
60E
120E
180
0 0.5 1 1.5 2 2.5 3 3.5 4

(b)

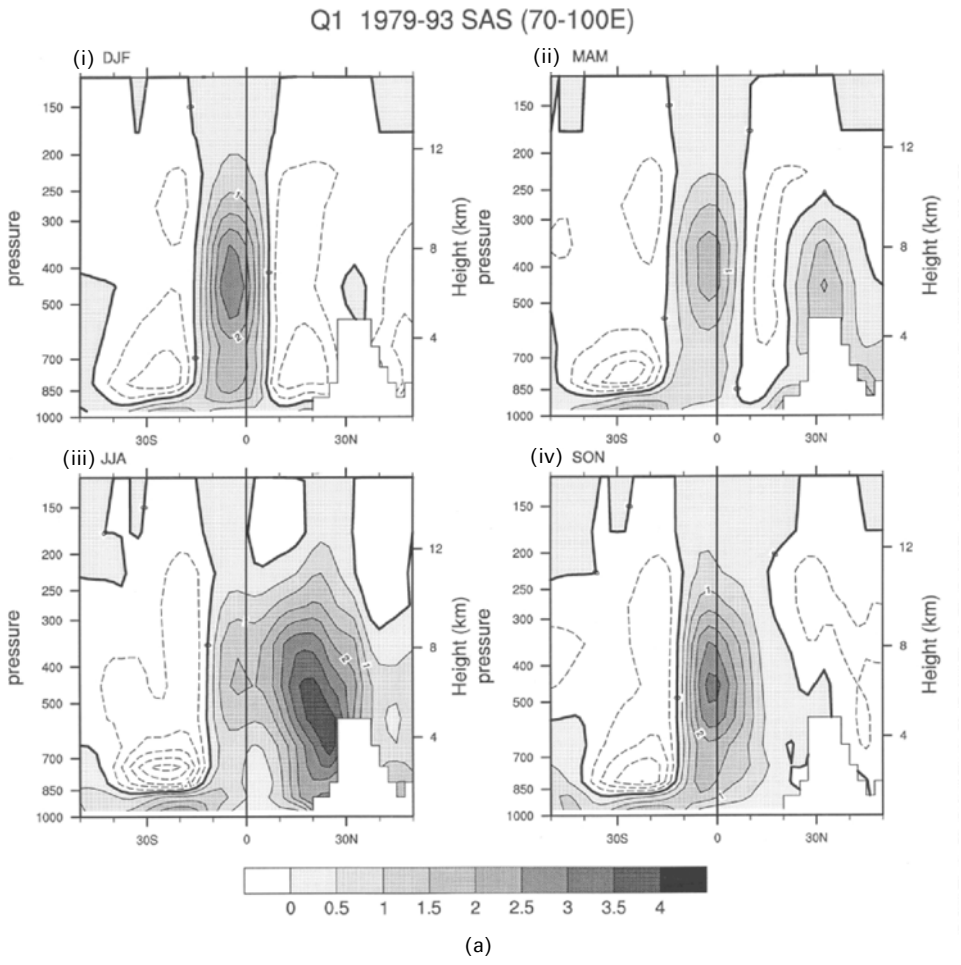

Figure 13.9. (a) Latitude–height sections of the 1979–1993 mean Q_1 for (i) DJF, (ii) MAM, (iii) JJA, and (iv) SON (K per day), averaged between 70°E and 100°E. (b) Similar to (a) but for the 1979–1993 mean Q_2.

Recently, the atmospheric response to different surface properties and vegetation has become an active area of research (e.g., Xue *et al.*, 2004).

Luo and Yanai (1984), Yanai *et al.* (1992), and Yanai and Li (1994) reported the observation of diurnal formation of a deep mixed layer (in terms of potential temperature) on the Tibetan Plateau (especially on the western Plateau) in the pre-monsoon period. The mixed layer was very deep at Shiquanhe (elevation 4,279 m) on the western Plateau (4-month mean top: near 400 hPa) and becomes shallower toward the central Plateau (Naqu) and the eastern Plateau (Jimai). They speculated on the role of 'dry plumes' rising from the heated surface. More detailed observations of the mixed layer formation were reported by Endo *et al.* (1994) using 1993

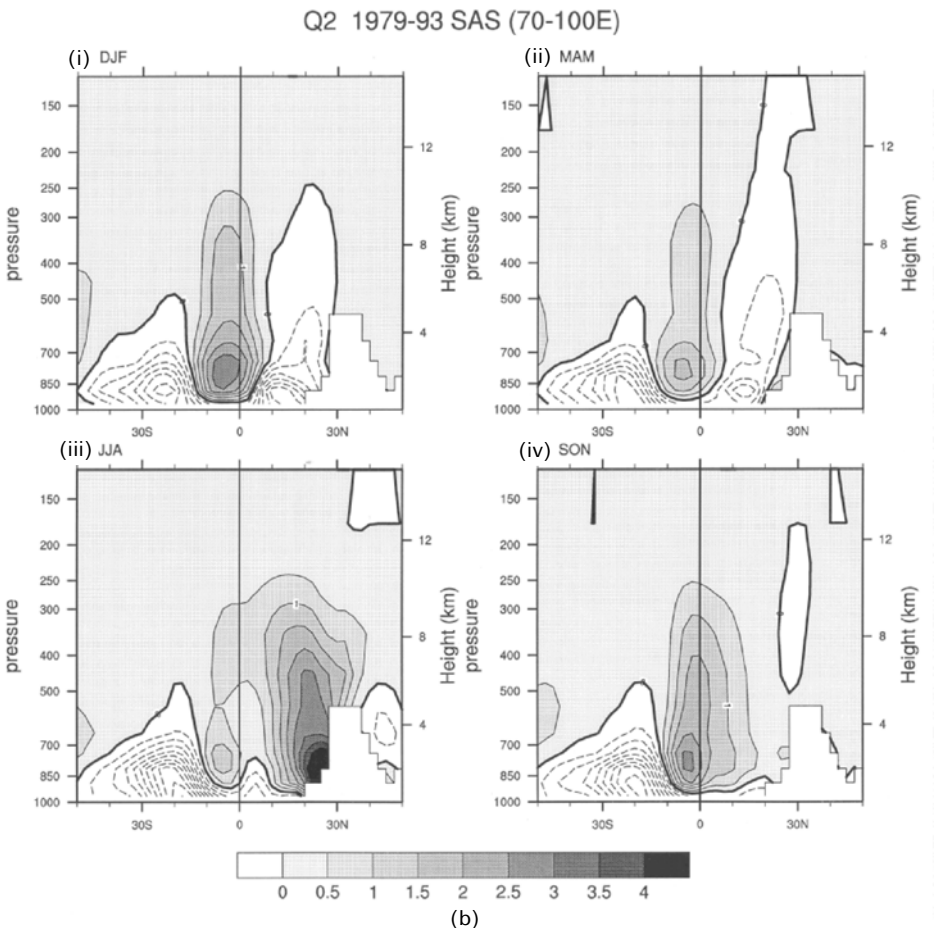

data and by Kuwagata *et al.* (2001) using the GAME–Tibet data. The behavior of the mixed layer is very similar to that found over the heated land such as the famous 'Wangara' boundary layer over Australia (Clarke *et al.*, 1971; Stull, 1988; Garratt, 1992).

We must be careful, however, in the interpretation of heating mechanism on the western Plateau. Satellite observation suggests that there are rains during the preonset period even on the western Plateau especially along the western and southwestern slopes, thus contributing to condensation heating (e.g., Ueda *et al.*, 2003a).

Luo and Yanai (1984), Yanai *et al.* (1992), and Yanai and Li (1994) also found that the mixing ratio q of water vapor is not well mixed and shows a decrease with height. Furthermore, q is smaller during the evening (1200 UTC) than in the morning (0000 UTC). This was confirmed by an extensive study by Kuwagata *et al.* (2001) using various data sources. Earlier, Mahrt (1976) reported similar observations in the high plains region of the USA and explained the decrease of moisture with height

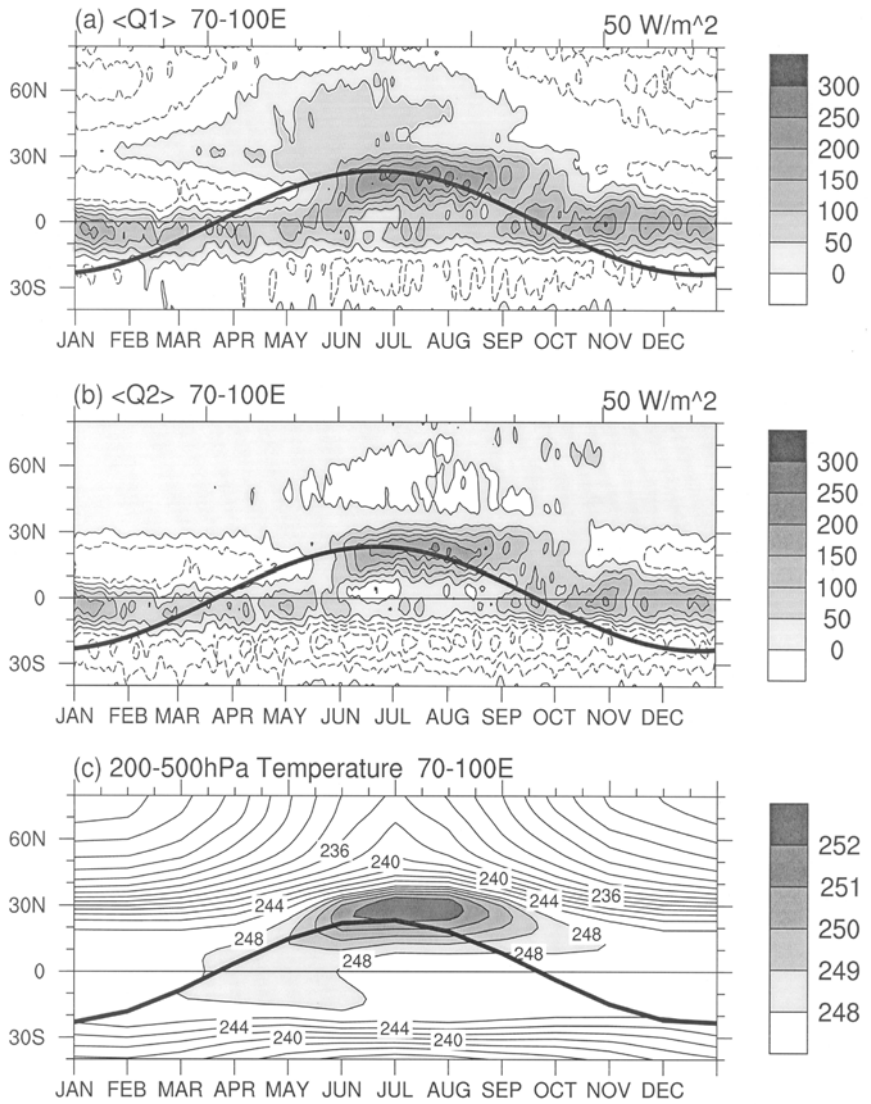

Figure 13.10. Time–latitude sections of the 1979–1993 mean (a) $\langle Q_1 \rangle$, (b) $\langle Q_2 \rangle$, and (c) upper tropospheric (200–500 hPa) temperature, averaged over 70°–100°E. The contour interval for (a) and (b) is 50 W m^{-2}. For (c) the contour interval is 1 K (2 K) when the values are larger (smaller) than 248 K. The thick solid curve is the solar declination angle.

as a result of entrainment of dry air aloft into the rapidly growing mixed layer (see also Mahrt, 1991). On the other hand, Kuwagata *et al.* (2001) considered this a result of local circulation because most of the sounding stations on the Tibetan Plateau are located in valleys.

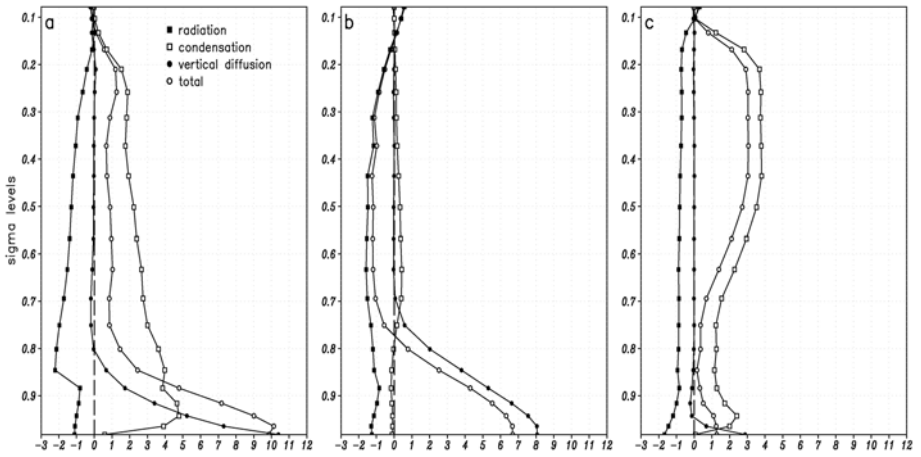

Figure 13.11. July mean area-averaged profiles of the total diabatic heating rate and its components over (a) the Tibetan Plateau region (75°–105°E, 27.5°–37.5°N); (b) middle Asia region (55°–70°E, 30°–42.5°N); and (c) east China region (110°–120°E, 27.5°–37.5°N). Units are K per day. Data are from the monthly mean NCEP/NCAR reanalysis from 1980–1999.

Our knowledge of the detailed heating mechanisms over the Tibetan Plateau is still limited. Although reanalysis data can provide temporal and spatial distributions of different components of heating (Figure 13.11) they are model dependent. More definitive observations are needed to resolve the various problems found by preliminary studies. Since the Topography Experiment for Ocean Circulation (TOPEX)/GAME–Tibet (1998) there have been extensive boundary layer, convection, and precipitation measurements over the Tibetan Plateau. Preliminary results from the field experiments and satellite observations, as well as numerical simulations, show some promise in clarifying these questions (e.g., Zhou *et al.*, 2000; Tanaka *et al.*, 2001; Ueno *et al.*, 2001; Uyeda *et al.*, 2001; Ma *et al.*, 2003; Yang *et al.*, 2003, 2004a,b).

13.4 THERMAL INFLUENCES OF THE TIBETAN PLATEAU ON THE SEASONAL TRANSITION OF CIRCULATION AND ASIAN MONSOON ONSET

13.4.1 Sensible heat driven air-pump over the Tibetan Plateau

Tao and Chen (1987) pointed out that due to the existence of the Tibetan Plateau, the east Asian monsoon onset occurs about two to three weeks earlier than the Indian monsoon onset. Wu and Zhang (1998) further showed that it is due to the mechanical as well as thermal forcing of the Tibetan Plateau that the Asian monsoon onset is composed of three consequential stages: the earliest over the eastern BOB to

the western Indo-China peninsula in early May. The BOB monsoon onset creates favorable conditions for the SCS monsoon onset in mid-May (Liu *et al.*, 2002). These lead to the great changes in both large-scale circulation and diabatic heating over Asia. Finally, the Indian monsoon onset appears in early June.

In Section 13.2, it is demonstrated that in winter the air over the Tibetan Plateau sinks in the free atmosphere (Figure 13.3(a) and (b)) and diverges from the Plateau to the surrounding areas near the surface (Figure 13.2(e)), whereas in summer it arises in the free atmosphere (Figure 13.3(c) and (d)) and converges from the surrounding areas to the plateau near the surface (Figure 13.2(f)). Using a nine-layer GCM, Wu and his collaborators (1997a, 1998, 2004) studied how the elevated heating of the Tibetan Plateau affects the local climate and global circulation. They indicated that due to the surface cooling in winter and heating in summer, the air column over the Tibetan Plateau descends strongly in winter and ascends strongly in summer. It acts as a huge air-pump and regulates the seasonal evolution of the lower layer circulation over the surrounding areas, contributing to the occurrence of the south Asian, BOB, SCS, and the western Pacific monsoons. However, were there no surface sensible heating, such an air-pump would not expel or suck the surface airflow. This is because in the absence of surface sensible heating, the surface air parcel has to stay on the same isentropic surface and cannot penetrate the surface downward or upward along the Tibetan Plateau slopes. In other words, such an air-pump must be driven by the surface sensible heating and is defined as the sensible heat driven air-pump, or SHAP for short (Wu *et al.*, 1997a, 2002b and Wu, 2004).

It is important to note that the SHAP affects not only the airflow near the surface, but also the circulation in the upper layers. As was discussed in Section 13.2, the Tibetan Plateau is a negative vorticity source in summer. Since in the upper troposphere the northern Tibetan Plateau is located within the westerlies, this negative vorticity source may trigger perturbations along the westerlies and affect the circulation anomalies. To verify this, numerical experiments were designed. The model used is the climate model Global–Ocean–Atmosphere–Land–System (GOALS) that was developed at the Laboratory of Atmospheric Sciences and Geophysical Fluid Dynamics (LASG), Institute of Atmospheric Physics (IAP) (Wu *et al.*, 1997b; Zhang *et al.*, 2000). Its atmospheric component (Wu *et al.*, 1996a) has 9 levels in the vertical and is rhomboidally truncated at wavenumber 15 in the horizontal. The ocean component (Zhang *et al.*, 1996) has 20 layers in the vertical with a horizontal resolution of 4° latitude by 5° longitude. The land component uses the simplified simple biosphere (SSiB) model (Xue *et al.*, 1991; Liu and Wu, 1997). The K-distribution scheme developed by Shi (1981) is used for the parameterizing radiation processes. This model has been used in the Atmospheric Model Intercomparison Program (AMIP), Coupled Model Intercomparison Program (CMIP), and Task I of the Intergovernmental Program for Climate Change (IPCC, 2001). There are two experiments in this study. In the first experiment, cloud distributions are prescribed using satellite remote sensing data for the calculation of radiation. There is no cloud–radiation feedback. The observed distributions of SST and sea ice from 1979 to 1988, which were set for the AMIP experiments, are introduced as the prescribed lower boundary conditions to integrate the model for 10 years. This is

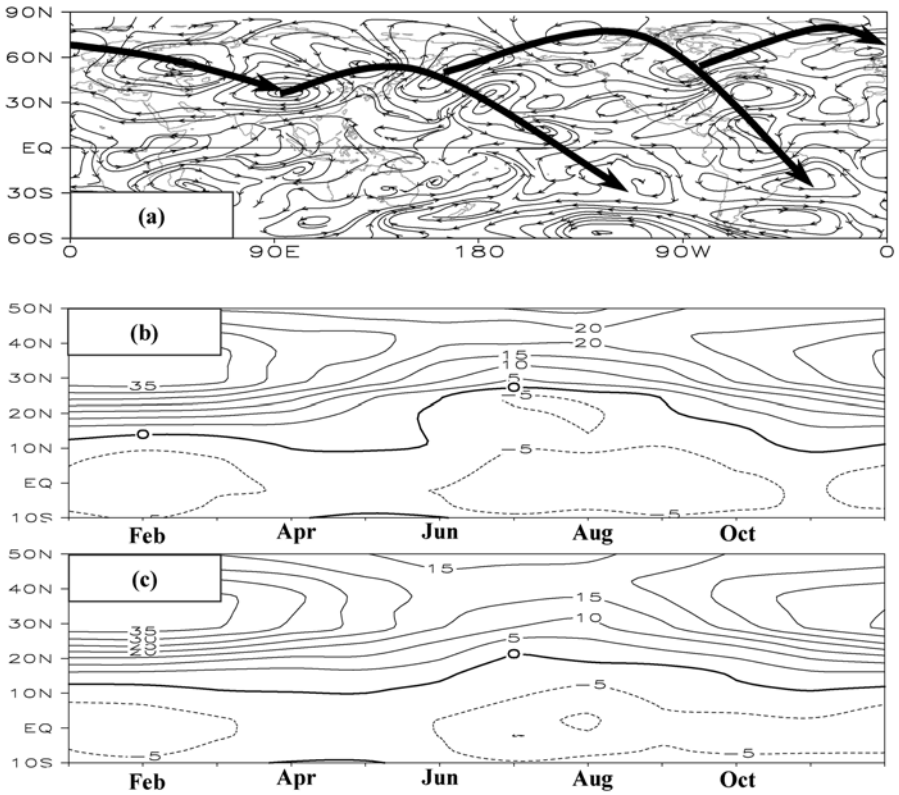

Figure 13.12. The difference of July mean stream field at 200 hPa between the experiments of CON and NSH (a), and the simulation results of the seasonal evolutions of the zonal wind u and the ridge line of the subtropical anticyclone ($u = 0$) along 90°E in the experiments CON (b) and NSH (c).

defined as the CON run. The second experiment is the same as the CON except that the sensible heating over the Tibetan Plateau region that is above 3 km is not allowed to heat the atmosphere aloft. This is achieved by switching off the sensible heating term in the thermodynamic equation at the grid points over the plateau region. This experiment is then defined as the NSH run. Since there is no cloud–radiation feedback in the model and the cloud amounts are prescribed, and since the ground surface temperature in the model is calculated based on the thermal equilibrium assumption, the energy budgets at the ground surface in the two experiments are kept unchanged. Therefore, the difference between the two experiments can be considered as resulting purely from the sensible heating over the plateau.

The difference in stream field at 200 hPa between CON and NSH shown in Figure 13.12(a) demonstrates that the sensible heating over the Tibetan Plateau does generate anticyclonic vorticity in the upper troposphere as was discussed in Section 13.2. More importantly, such a sensible heat-induced vorticity source over the Plateau forces a series of stream field anomalies in the form of a ray of Rossby

waves. Although this result is obtained through numerical experimentation, it is also supported by observational evidence. Based on the NCEP/NCAR monthly mean data, Liu X. *et al.* (2002) analyzed the correlation between the July heating over the Tibetan Plateau area and the corresponding 200-hPa geopotential height, and obtained a similar pattern of Rossby wave rays. This implies that the effective working of the SHAP over the Tibetan Plateau affects not only the climate anomaly in the surrounding area but also the circulation over the northern hemisphere.

Furthermore, such a SHAP has significant impacts on the seasonal transition of the atmospheric circulation at least over the Asian monsoon areas. Yeh *et al.* (1959) found that the seasonal transition between winter and summer patterns is abrupt: in late May and early June, the westerly jet retreats quickly from the south of the Tibetan Plateau to its north, and the associated ridge line of the subtropical anticyclone and the circulations over south Asia also jump northward; whereas in October the circulation experiences the opposite abrupt seasonal transition. These abrupt seasonal transitions are closely linked with the Asian monsoon onset and retreat. In Figure 13.12(b) and (c) are demonstrated the seasonal evolutions of the 500-hPa zonal wind at 90°E based on the results of the aforementioned numerical experiments CON and NSH, respectively. In CON, in which the surface sensible heating over the Tibetan Plateau exists (Figure 13.12(b)), the easterly axis in winter is maintained near the equator, the westerly axis at 35°N, and the ridge line of the subtropical anticyclone identified by $u = 0$ near 12°N. By the end of May and early June, the tropical easterly axis suddenly jumps northward, the westerly axis settles to the north of the Tibetan Plateau at about 42°N, and the abrupt change in the location of the ridge line of the subtropical anticyclone is the most evident. In October, the seasonal transition in circulation experiences the opposite direction. All this is in good agreement with Yeh *et al.* (1959). On the other hand, in the experiment NSH, in which the sensible heating over the Tibetan Plateau area where elevation is above 3 km is not allowed to heat the atmosphere, the seasonal transition between the winter and summer patterns becomes smooth, and the abrupt transition disappears (Figure 13.12(c)). This is because the strong surface sensible heating over the Tibetan Plateau and the strong latent heat release associated with the east Asian monsoon in May greatly intensify the SAH (Wu *et al.*, 1999; Liu Y. *et al.*, 1999, 2001). As a result, the wintertime westerlies to the south of the Tibetan Plateau are substantially weakened, whereas the westerlies to its north are intensified – abrupt changes in circulation thus occur. After the withdrawal of the Asian monsoon, the SAH is weakened, and the circulation returns to its winter pattern.

13.4.2 Thermal impacts of the Tibetan Plateau on seasonal transition and Asian monsoon onset

As demonstrated in Figure 13.10(a), during the spring months while the Tibetan Plateau domain has become a heating region, the areas over the Indian Ocean to its south and over the land surface to its north are still experiencing cooling. The heating over the Tibetan Plateau starting from early spring will then help the over-

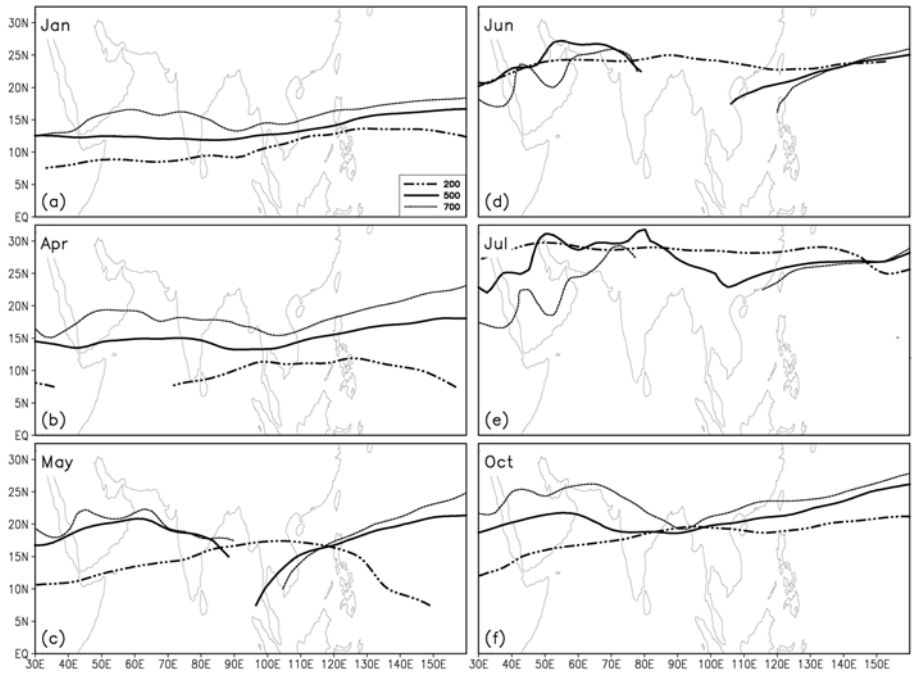

Figure 13.13. Distributions in different months of the ridge lines of the subtropical anticyclone at 700 hPa (dashed curve), 500 hPa (solid curve), and 200 hPa (dotted curve) averaged from 1980 to 1997.

turning of the meridional temperature gradient in the region (Figure 13.10(c)) in favor of the Asian monsoon onset (Flohn, 1957; Li and Yanai, 1996). This can be viewed by diagnosing the configuration of the subtropical anticyclone ridge surface.

In winter months from October to April, the ridge lines of the subtropical anticyclone in the troposphere are all zonally located (Figure 13.13). These ridge lines then comprise a surface. It becomes a continuous boundary that separates the westerlies to the north and the easterlies to the south, and can be defined as WEB (westerlies and easterlies boundary) for short. On the other hand, the tilting of the WEB can be measured by the vertical shear of zonal wind across the WEB surface (i.e., $\partial u/\partial z$). Subject to the thermal wind relation, the reversal of meridional temperature gradient across the WEB must be accompanied by a change in vertical tilting of the WEB. In winter, the tropical air temperature to the south of the WEB is warmer than to its north, and the WEB surface tilts southward with increasing height (Figure 13.13). In summer, the Asian continent to the north of the WEB is warmer than the ocean to its south. As a result, the sector of the WEB surface over the Asian monsoon area tilts northward, while other parts of the WEB surface still keep tilting southward. The lower part of the WEB surface is then broken. Therefore, the monsoon onset index of the reversal in the prevailing wind direction in the lower troposphere can be viewed as the breaking of the lower part

of the WEB where the wintertime easterlies to the south of the WEB are replaced by westerlies after the monsoon onset. Figure 13.13 indicates that on monthly scales the onset of the Asian monsoon is in May and its withdrawal is in October.

When the ridge lines at different levels intersect at one point (e.g., Point C or D in Figure 13.14), the WEB surface at that point becomes perpendicular to the Earth's surface. The vertical axis at this point on the surface can then be defined as a seasonal transition axis, or STA for short. The appearance of an STA then implies the start of the seasonal transition. Since it is usually accompanied by the occurrence of severe convective rainfall, it is also the time of monsoon onset. Figure 13.14 shows the pentad-mean evolution of the ridge lines at different levels calculated from the NCEP/NCAR reanalysis and averaged from 1980 to 1997 (Mao *et al.*, 2002a and b). Before the end of April (Figure 13.14(a–d)), the ridge lines from 700 hPa upwards all tilt southward with increasing height, presenting a typical winter pattern. By 1–5 May (Figure 13.14(e)), the WEB surface becomes perpendicular between point C (105°E) and point D (90°E) along 12°N, just over the eastern BOB and western Indo-China peninsula, and the 850-hPa wind direction south of 12°N over the BOB area has changed from easterly to westerly, indicating the BOB monsoon onset. Afterwards, the STA point C propagates eastward quickly. By 16–20 May (Figure 13.14(h)), it reaches the eastern SCS, and the wind directions at 850 and 700 hPa to the south of 16°N over most of the SCS have been overturned from easterly to westerly. This corresponds to the SCS monsoon onset. The arrival of the STA point C by 135°E in early June (Figure 13.14(k)) is well coordinated with the western Pacific monsoon onset (Wang and Lin, 2002). Meanwhile, the STA point D moves westward gradually. By early June, it arrives in western India (Figure 13.14(k) and (l)), in accordance with the Indian monsoon onset. By this time, the monsoon onset procedure is completed, and the summer circulation pattern over Asia is established. These results are also in good agreement with the results of Wu and Zhang (1998) that the Asian monsoon onset continues for about forty days, and is composed of three consequential stages: the earliest in the early May over the eastern BOB, then the SCS monsoon onset by 20 May, and the Indian monsoon onset in early June. They showed that in early spring, partly due to the Tibetan Plateau heating and the westerly advection over the plateau, the air over its eastern part is warmer than over its western part. The meridional thermal contrast between the eastern part of the Tibetan Plateau in the north and the North Indian Ocean in the south then becomes strongest. This is in favor of the earliest overturning of the meridional temperature gradient over the eastern part of the BOB and the western Indo-China peninsula. Therefore, the Asian monsoon onset occurs firstly over this area.

To verify this result, the time series of the BOB monsoon onset is constructed for the BOB domain (90°–100°E, 5°–15°N) based on the following criteria:

(a) The meridional temperature gradient ($\partial T/\partial y$) across the WEB surface has changed its sign from negative to positive and maintained this change for 5 consecutive days;
(b) The vertical shear of the zonal wind ($\partial u/\partial z$) across the WEB surface has changed its sign from positive to negative; and

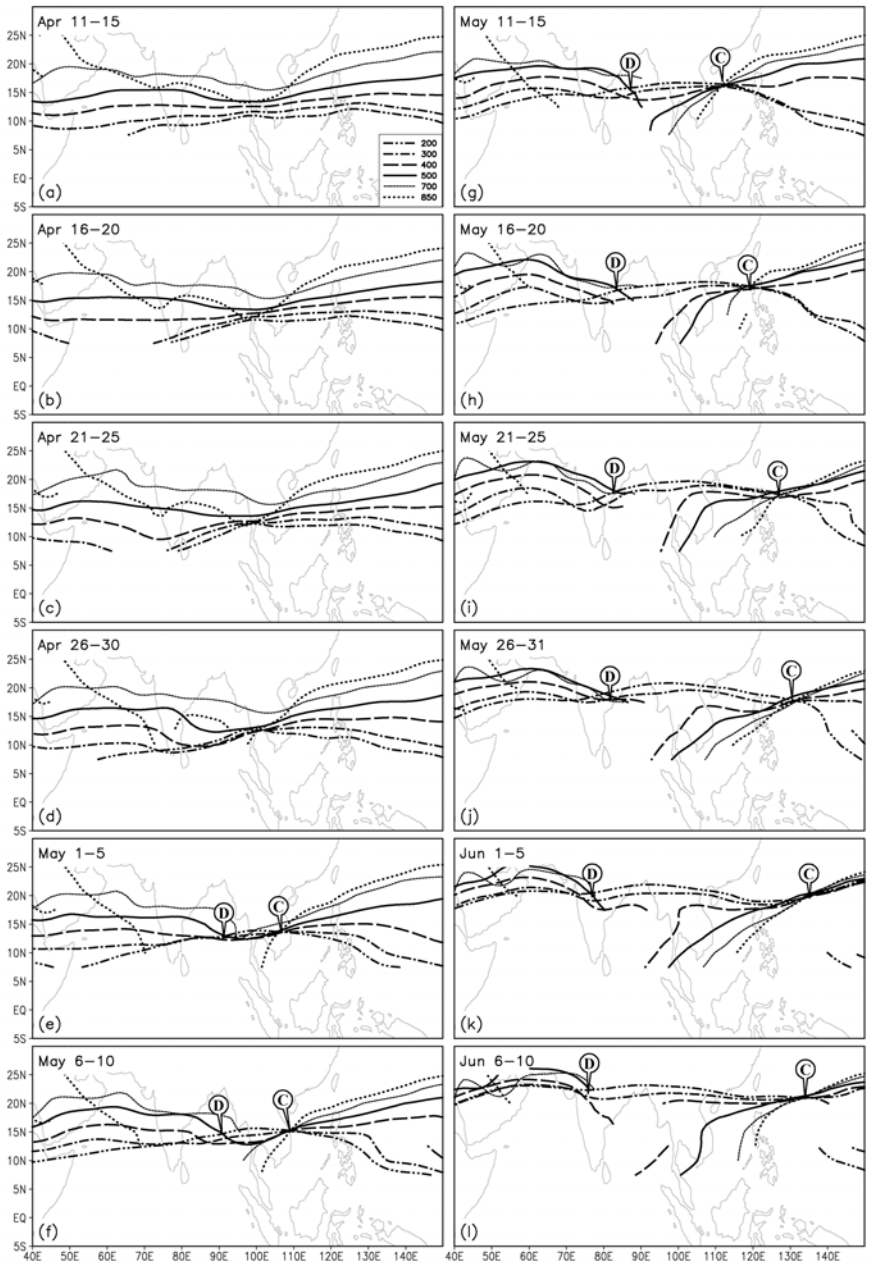

Figure 13.14. The projection of the subtropical anticyclone ridge line ($u = 0$) at the levels from 850 hPa to 200 hPa during the season transition (from the third pentad of April to the second pentad of June) (a) 11–15 April, (b) 16–20 April, (c) 21–25 April, (d) 26–30 April, (e) 1–5 May, (f) 6–10 May, (g) 11–15 May, (h) 16–20 May, (i) 21–25 May, (j) 26–31 May, (k) 1–5 June, (l) 6–10 June.

(c) The outgoing long-wave radiation (OLR) at the site under examination has decreased to below 230 Wm^{-2}.

This time series of the BOB monsoon onset is then used to calculate its time lag correlations with temperature and geopotential height fields. Figure 13.15 displays the time lag correlation between the BOB monsoon onset and the monthly mean geopotential height at 200 hPa, in which the statistically significant correlation higher than 95% is shaded. It shows that in the years with early/late BOB monsoon onsets, the 200-hPa monthly mean geopotential heights over the Tibetan Plateau before the onset (from December to April) are continuously higher/lower than normal. In other words, the warmer the air over the eastern Tibetan Plateau, the earlier the BOB monsoon onset. This result supports our earlier conclusion that the Tibetan Plateau heating in spring contributes substantially to the earliest monsoon onset over the eastern BOB and western Indo-China peninsula.

13.5 CONCLUDING REMARKS

In this chapter, we have briefly reviewed the study of the effects of the Tibetan Plateau during the last half century. However, there are issues this chapter did not discuss because of textual extent limitations. These include:

- **The effects of mountain uplift**
  Raising the altitude of large-scale mountains can increase the non-linear atmospheric response to mechanical forcing and planetary waves (Wu, 1984; Trenberth and Chen, 1988). Early GCM results with and without an account of mountains (e.g., Hahn and Manabe, 1975; Kutzbach *et al.*, 1989) established the role of mountains in enhancing the Asian monsoon. Liu and Yin (2002) showed that the evolution of the east Asian monsoon may be more sensitive to the uplift of the Tibetan Plateau than that of the south Asian monsoon. Recently, Abe *et al.* (2004) and Kitoh (2004) used a coupled atmosphere–ocean GCM and showed that the mountain uplift causes changes in the SST of the surrounding oceans, resulting in a larger sensitivity of the east Asian monsoon to the uplift than previously obtained using the atmospheric GCM alone.
- **The effects of snow cover**
  Many observational studies and GCM experiments (e.g., Hahn and Shukla, 1976; Barnett *et al.*, 1989; Yasunari *et al.*, 1991) examined the relationship between the Eurasian–Tibetan Plateau snow cover and the subsequent Asian monsoon. An inverse relation between the winter snow cover and the subsequent summer monsoon rainfall was generally noted. However, a detailed study (Bamzai and Shukla, 1999) revealed that western Eurasia is the region for which a significant inverse correlation exists between winter snow cover and subsequent summer monsoon rainfall. They did not find a significant relation between the Himalayan snow cover and subsequent monsoon rainfall. Ueda *et al.* (2003b) studied factors contributing to the spring northward retreat of

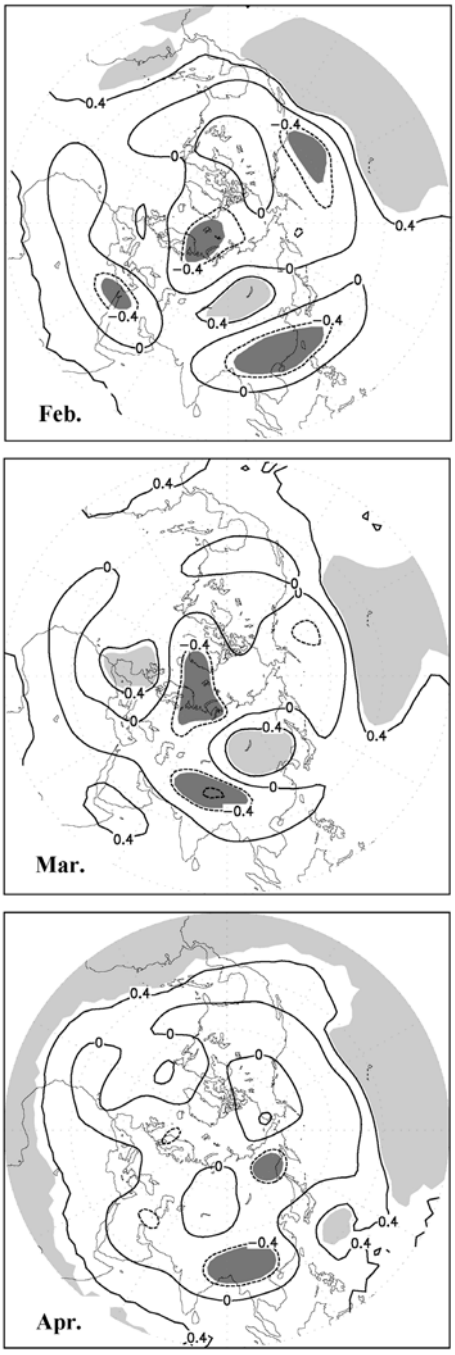

Figure 13.15. The time lag correlation coefficients between the monsoon onset over the eastern part of the BOB and the monthly mean 200-hPa geopotential height.

Eurasian snow cover. They showed that the surface air temperature anomalies produced during the snow disappearance period diminishes in May, suggesting a rather weak dynamic link between the snow cover and Asian summer monsoon. Recently, Zhang *et al.* (2004) discussed the decadal change of spring snow depth over the Tibetan Plateau and its influence on the east Asian summer monsoon.

- **Climatic warming**
  Liu and Chen (2000) discussed the observed warming trend over the Tibetan Plateau during recent decades. Chen *et al.* (2003) made a model study of the climatic warming in the Tibetan Plateau due to a doubling of CO_2.

Now we can make brief conclusions about the studies on the effects of the Tibetan Plateau. Mechanically the Tibetan Plateau, representing a huge obstacle, can block atmospheric basic flows and split the wintertime westerlies into the northern and southern branches. It also has a dominant effect on lee cyclogenesis and associated northerly cold surges in winter. Since Ye h *et al.* (1957) and Flohn (1957) discovered the heating nature of the Tibetan Plateau, a new field of research (i.e., the Tibetan Plateau meteorology) has been established. During the past decades, many efforts have been devoted to understanding its heating features and the consequent weather and climatic impacts. Much new light has been shed on the associated mechanisms. It has become certain that the Tibetan Plateau is a heat sink in winter but a heat source in summer. Recent studies also show that the Tibetan Plateau is a strong negative vorticity source in summer, which, via energy dispersion, affects the anomaly of the atmospheric circulation at least in the northern hemisphere. Strong descending in winter and ascending in summer of the air column over the Tibetan Plateau represents a huge air pump, and regulates the annual cycle of the global circulation and the monsoon climate over Asia, Africa, and Australia. Furthermore, due to it having a larger 'memory' than the underlying surface, the Tibetan Plateau heating in late winter and spring can exert both simultaneous and delayed impacts on the weather and climate anomalies in summer in the surrounding areas (Chen and Yan, 1981; Wu *et al.*, 1996a,b; Hsu and Liu, 2003), and can be used as a prediction indicator.

However, most of these conclusions are still qualitative in nature. Our further understanding on the Tibetan Plateau forcing and its impacts on weather and climate are hampered by various limitations. First of all the sparseness and the lack of representativeness in observational data over the complex topography shadows the heating details over the plateau. Due to a lack of knowledge about the land–air–sea interaction in this area, questions concerning how the Tibetan Plateau and its heating nature affect the local and global climate remain unclear, and the use of such a knowledge for quantitative climate prediction is still unavailable. To move forward, we need to plan our coordinated research to take in many aspects, such as:

- Expanding our understanding from summer months to other months. Most of the existing research is focused on the impact of the Tibetan Plateau on circulation and climate in the summer months. To achieve a coherent understanding we need to study how the Tibetan Plateau cooling in winter affects the weather and

climate, and how the annual variation of the Plateau heating is associated with the seasonal evolution of the atmospheric circulation.

- Revealing all the mechanisms related to the Asian monsoon onset. The climate system is a non-linear, dissipative, and open system, and the timing and location of the Asian monsoon onset is influenced by many factors not just the Tibetan Plateau heating, such as the persistently external forcing and low-frequency oscillations in the atmosphere (e.g., the MJO).
- Detailing the heating feature over the Tibetan Plateau. Up to now, our knowledge of the Tibetan Plateau heating is rather limited. Although reanalysis data can provide temporal and spatial distributions of different heating, they are model dependent. The provision of vertical profiles of different heating over the Tibetan Plateau and its neighboring regions will enable the study of the circulation formation and its impacts on regional as well as global climate.
- Analysing the response of the Tibetan Plateau thermal status to global change. Most of the existing research concerns how the Tibetan Plateau thermal status affects the global climate. However, the changes in global climate will in return influence the thermal status over the Tibetan Plateau and its contrast with those over the Indian Ocean and western Pacific, eventually exerting different forcing on the global climate.
- Revealing the physical processes associated with the interactions between the Tibetan Plateau and the atmosphere. To achieve this, more field observation experiments and numerical modeling are required.

All these and other related research issues demand great efforts and will continue in the coming decades.

13.6 ACKNOWLEDGEMENTS

We would like to thank Professor Duzheng Ye for his help and encouragement during writing. Thanks are also due to the editor, and to Professor T. Murakami, Dr. Akio Kitoh, and Dr. Jun Matsumoto for kindly offering useful comments and help on improving our original draft. The first author thanks Drs. Chih-wen Hung, Xiaodong Liu, and Hui Su for their useful discussions and assistance with the illustrations; the second author thanks Drs. Xin Liu, Jiangyu Mao, and Anmin Duan for producing the relevant figures. This work was partially supported by the Chinese Academy of Sciences under Grant No. ZKCX2-SW-210, the National Natural Science Foundation of China under Grant Nos 40135020 and 40475027, the National Oceanic and Atmospheric Administration under Grant NA96GP0331, and by the National Science Foundation under Grant ATM-9902838.